LAWRENCE
LIVERMORE
NATIONAL
LABORATORY

LLNL-TH-631353

Development of aerogel-lined targets for inertial confinement fusion experiments

T. Braun

March 28, 2013

Disclaimer

This work performed under the auspices of the U.S. Department of Energy by Lawrence Livermore National Laboratory under Contract DE-AC52-07NA27344.

PHYSIK-DEPARTMENT

Development of aerogel-lined targets for inertial confinement fusion experiments

Diplomarbeit

von

Tom Braun

TECHNISCHE UNIVERSITÄT MÜNCHEN

LLNL-TH-631353

Abstract

This thesis explores the formation of ICF compatible foam layers inside of an ablator shell used for inertial confinement fusion experiments at the National Ignition Facility. In particular, the capability of p-DCPD polymer aerogels to serve as a scaffold for the deuterium-tritium mix was analyzed. Four different factors were evaluated: the dependency of different factors such as thickness or composition of a precursor solution on the uniformity of the aerogel layer, how to bring the optimal composition inside of the ablator shell, the mechanical stability of ultra-low density p-DCPD aerogel bulk pieces during wetting and freezing with hydrogen, and the wetting behavior of thin polymer foam layers in HDC carbon ablator shells with liquid deuterium.

The research for thesis was done at Lawrence Livermore National Laboratory in cooperation with the Technical University Munich.

Table of Contents

1 Introduction

In a world with an increased demand for energy [1-4], nuclear fusion, the sun's energy source, is a potential promising candidate to contribute to the global energy mix [5-11]. One advantage of nuclear fusion reactions over traditional chemical reactions is the high energy density. For example, the energy released during a deuterium-tritium-reaction is 17.6 MeV[1], whereas the energy required to ionize atomic hydrogen is just 13.6 eV. Deuterium-tritium-reactions have the advantage over other possible fusion reactions of a high energy output and a large cross-section at feasible temperatures and are, therefore, used for most fusion based experiments.

To achieve controlled nuclear fusion reactions for energy research and high density physics experiments, the Lawson criterion has to be fulfilled, which states "that not only must the temperature be sufficiently high, but also the reaction must be sustained long enough for a definite fraction of the fuel to be burnt."[12, 13] Therefore, the plasma needs to be confined so that the product of temperature and pressure necessary for the fusion reaction reaches the threshold. Two approaches to confine the plasma are considered: Magnetic Confinement and Inertial Confinement.

1.1 Magnetic Confinement Fusion

Magnetic confinement fusion uses magnetic fields to confine the energy by influencing the movement of the charged particles within the plasma. The Lorentz force holds the particles close to the magnetic field lines, since charged particles can only move freely along the magnetic field lines. Two of the most

[1] D + T => ^{4}He (3.5 MeV) + n (14.1 MeV)

advanced geometrical designs are the tokamak[14] and stellarator[15] design. The tokamak reactor is a torus in which the ring is surrounded by electromagnets that create a toroidal magnetic field and uses an induced plasma current to create a poloidal field. The combination of the two fields prevents the drift of particles across the magnetic field allowing a stable plasma equilibrium. The plasma is confined long enough to allow the deuterium and tritium to fuse and produce energy. To start the fusion reaction deuterium and tritium is injected into the evacuated reactor vessel and heated to 10^8 K by different methods such as ohmic heating, magnetic compression[16, 17], high frequency plasma heating[18], or neutral beam injection. Once the product of temperature and pressure is high enough, the ^{4}He particles heat the plasma so that the reaction is self-sustaining. The ^{4}He particles and additional particles escaping the confinement need to be removed by a divertor[14, 19, 20]. The other possibility to create the helical twisting of field lines is the stellarator concept, which uses exclusively external coils to create the magnetic field. This theoretically allows continuous operation and also prevents potential instabilities caused by the plasma current. JET in Culham, United Kingdom and ASDEX Upgrade in Garching, Germany are tokamaks currently in operation. ITER, an experimental tokamak reactor, in Caderache, France is currently in the process of construction. Wendelstein 7-X, an experimental stellarator, is also currently being built in Greifswald, Germany.

1.2 Inertial Confinement Fusion

In inertial confinement fusion experiments, on the other hand, a solid or liquid deuterium-tritium mixture is compressed and heated to 10^8 K until the product of temperature and density is high enough, that the reaction reaches the Lawson criterion. One approach to reach the high densities, that are required, was published by Nuckolls et al.[10, 21]. They suggested a spherical implosion of a microsphere filled with the deuterium-tritium-mixture. This microsphere is commonly referred to as a ‘target’. The target is

usually compressed by a high-powered laser or ion beam, which hits the deuterium-tritium mixture symmetrically from all sides. This causes the ablator, the outer layer of the target, to vaporize in an outward direction, creating a reaction force, which accelerates the residue of the target in the opposite inward direction. The compressed deuterium-tritium mixture is extremely densified and heated up, causing the atoms to fuse. The confinement time is short enough that the inertia of the plasma itself is enough to confine it, leading to the name inertial confinement fusion.

In ion beam driven inertial confinement fusion experiments[22-25] a high energy beam of ions deposits its energy in the target, causing the fuel inside to compress and to ignite through shock implosion. Two possible concepts are heavy ion beams[24, 26] or light ion beams[23]. Profiles of density, temperature and pressure at different times are explained in depth by R.C. Arnold and J. Meyer-ter-Vehn[24].

Most of the concepts developed for laser driven inertial confinement fusion experiments propose hollow spheres as a target with different layers one the inside, one of them made of cryogenic deuterium-tritium[27-29]. A time shaped laser pulse is shot on the target in such a way that isentropic compression is achieved. The target is compressed in less than 10^{-9} s to densities of the order 10^{3} times of solid hydrogen until the Lawson criterion is fulfilled and ignition conditions are reached. If the laser is not shot directly onto the target, but into a hohlraum surrounding the target, the laser light is converted into X-rays, which

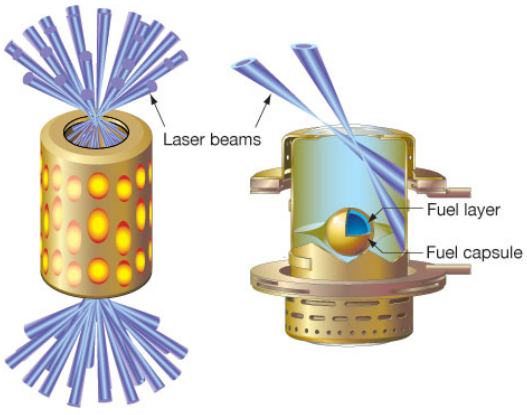

Figure 1: Indirect drive approach to inertial confinement fusion: The energy of the laser is directed inside a hohlraum, converting the light into X-rays, which are compressing the target. Source: NIF.

are compressing the target and ignite a fusion reaction. One of the advantages of this *indirect drive* approach is that the X-rays are causing a more symmetric implosion of the target. A very detailed comparison of direct drive and indirect drive approaches was done by C. Orth[30]. The indirect drive approach is currently used at the National Ignition Facility (NIF), Lawrence Livermore National Laboratory.

1.2.1 NIF

The National Ignition Facility at Lawrence Livermore National Laboratory, California, is the largest and most powerful inertial confinement fusion research facility built to date. NIF's laser is split into 192 beams, amplified and delivers 1.8 MJ of ultraviolet light into the target chamber (figure 2).

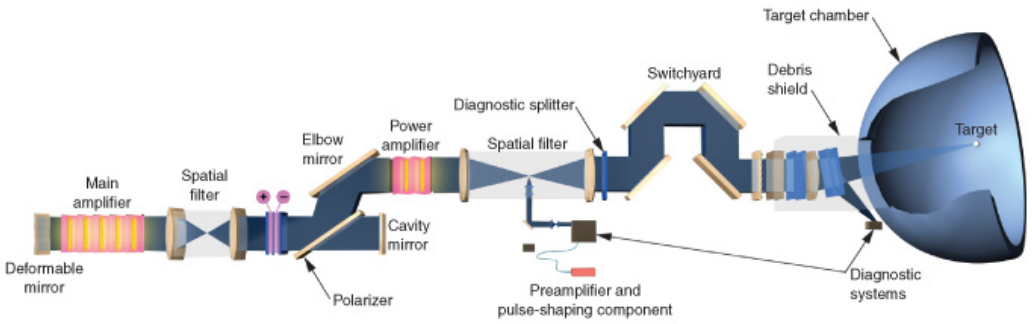

Figure 2: Components shape, smooth, and amplify the laser pulses generated by the National Ignition Facility's (NIF's) 192 beam lines, which all converge in the target chamber. Source: LLNL.

As mentioned above, NIF currently uses an indirect drive approach to heat and compress the target. Therefore not all energy from the laser reaches the target itself. Only roughly 75% of the energy is converted into X-rays and, due to heating of the hohlraum to temperatures of 250-300 eV or X-rays that escape, only 150 kJ reach the target.[31] The target is heated to more than 10^6 K and densified to roughly 1000 g/cc creating energies on the order of 10 to 35 MJ[32].

1.2.2 Foam lined ignition targets

In order to take full advantage of the unique laboratory environment that is created by the National Ignition Facility complex target structures are necessary. Guided by computer simulations numerous target designs have been developed and reported to the literature.[33, 34] One approach for direct drive fusion targets, which was first reported by R. A. Sacks, is “the use of a small pore size, open cell, rigid foam structure as a sponge to precisely define the [fuel] layer contours and to stabilize the liquid against gravitational slumping.”[35] The foam can act as surrogate to simulate the cryogenic fuel layer, which requires the foam to have a density similar to the deuterium-tritium at 14K (roughly 250 mg/cc) and a thickness comparable to the deuterium-tritium ice layer (roughly 60 μm). It simulates the mass effect of deuterium-tritium ice to measure the implosion velocity. In targets that have the deuterium-tritium-mixture, an additional advantage for having a foam layer inside these targets is that it permits bringing dopants in direct contact with the deuterium-tritium-fuel. The third, future target type, which has a foam layer inside, uses the foam to define the distribution of cryogenic deuterium-tritium, and should thus have the same thickness than the deuterium-tritium ice layer. The density should not exceed 10% of the density of cryogenic deuterium-tritium (25 mg/cc).

Different concepts of spherical foam targets based on R. A. Sack’s concept have been developed for direct drive fusion experiments.[36-44] These approaches, however, are difficult, if not impossible, to extend to the foam shells required for indirect-drive NIF ignition targets, as they require thinner and lower-density foam shells in combination with a much thicker ablator shell (> 80 μm instead of the only few μm-thick polymer permeation barriers used in direct-drive targets). Beyond diagnostics and nuclear physics applications, foam-lined targets with thicker foam layers also have the potential to greatly facilitate the fabrication of smooth and homogeneous DT fuel layers for indirect-drive ICF experiments.[45]

2 Experimental Results

This thesis explores the formation of ICF compatible foam layers inside of an ablator shell used for inertial confinement fusion experiments at the National Ignition Facility. In particular, the capability of p-DCPD[46, 47] polymer aerogels to serve as a scaffold for the deuterium-tritium mix was analyzed. Four different factors were evaluated: the dependency of different factors such as thickness or composition of a precursor solution on the uniformity of the aerogel layer, how to bring the optimal composition inside of the ablator shell, the mechanical stability of ultra-low density p-DCPD aerogel bulk pieces during wetting and freezing with hydrogen, and the wetting behavior of thin polymer foam layers in HDC carbon ablator shells with liquid deuterium.

2.1 Uniformity dependency

One of the most important requirements for inertial confinement fusion experiments is a symmetric implosion of the target. Imperfections in the foam layer could seed Rayleigh-Taylor instabilities leading to a non-symmetric implosion.[48-51] The Rayleigh-Taylor instability growth on low-density foam targets has been extensively studied[52], stating that a uniform polymer foam layer is essential for successful inertial confinement fusion experiments. Therefore, the dependency of different factors on the uniformity of the aerogel layer was analyzed. For these experiments thin layers of different DCPD compositions were formed under shear with specific predetermined conditions and compared to each other to find the best configuration to form thin film layers.

The coating experiments were performed in rotating vial geometry with a low profile roller (Stovall Life Science). This allowed simulating coating conditions under shear in a controlled environment, which is close to the coating process of the targets.

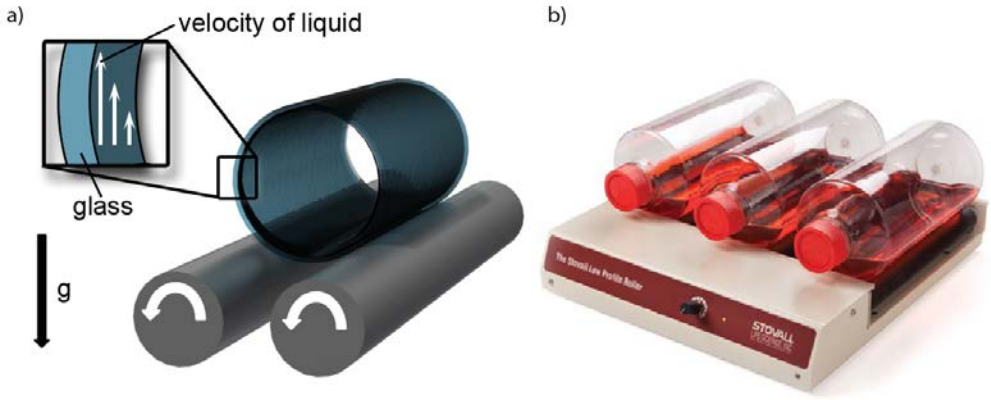

Figure 3: a) Schematic presentation of the shear flow caused by the velocity gradient, which is caused by the interplay of friction and gravity; b) representative picture of the experimental setup: glass vials were filled with a precise amount of precursor solution and placed on the roller to simulate shear conditions.

The vials (10 ml ampoule, clear, pre-scored, 17.6 mm inner diameter, Wheaton Industries) were filled with the necessary amount of gel precursor solution to get the desired layer thickness, sealed with Parafilm M or Polytetrafluoroethylene-Copper-sealant tape (Graigner) to prevent evaporation and rotated at 11 rpm during gelation.

Dicyclopentadiene (DCPD, $C_{10}H_{12}$, Aldrich), norbornene (NB, C_7H_{10}, 99%, Aldrich), and Grubbs' 1st generation catalyst, bis(tricyclohexylphosphine)benzylidene ruthenium (IV) dichloride (+97%, Aldrich) were used as received without further purification. As supplied, the DCPD monomer is predominantly *endo* isomer and contains butylated hydroxytoluene as stabilizer. Toluene (anhydrous, 99.8%, Aldrich) was purged with nitrogen gas prior to use. Poly(dicyclopentadiene-*random*-norbornene) (P(DCPD-*r*-NB)

gels were prepared from ring opening metathesis polymerization (ROMP)[46, 53-56] of DCPD and NB in toluene with Grubbs' 1st generation catalyst[57]. Density of the P(DCPD-*r*-NB) aerogels and gelation time were adjusted by the DCPD/NB-to-toluene and the DCPD/NB-to-catalyst ratio, respectively. For example, 50 mg/cc P(DCPD-*r*-NB) aerogels with 10 wt.% NB (relative to PDCPD) and 0.2 wt.% Grubbs' 1st generation catalyst were prepared by mixing 10 mL of a 50 mg/cc DCPD/toluene solution with 1 mL of a 50 mg/cc NB/toluene solution and adding 0.5 mL of a 2 mg/cc catalyst/toluene solution.

The uniformity of the wet gel layer was determined by optical analysis. To compare the obtained results a uniformity scale with arbitrary units reaching from 1 to 5 was developed, where 1 represents a low quality wet gel layer with a high number of irregularities (figure 5a) and 5 represents a uniform, almost transparent, film layer (figure 5b).

2.1.1 Norbornene and catalyst concentration

The first experiment conducted was the analysis of the pure DCPD's capability to withstand shear forces during gelation. For this purpose a vial was filled with 500 µl of a 25 mg/cc precursor solution, sealed, and rotated on the low profile roller for 24h at 11 rpm to analyze the uniformity. These initial tests revealed that pure DCPD does not form a uniform wet gel layer if gelled under the influence of shear[58], but instead forms lumps as seen in figure 5a. This indicates that the initially weak gel network is broken up by the applied shear forces during rotation. The effects of copolymerization with norbornene on the gelation behavior of DCPD-based polymer aerogels were therefore systematically evaluated. Norbornene has the advantage that it only forms linear chains and as a result reduces the amount of DCPD's cross linking functionality, which delays gelation and thus increasing the viscosity at the gel-point[58], strengthening the gel network. Increasing the viscosity at the gel point decreases the shear experienced by the forming gel which could increase the uniformity of the wet gel layers.

The gelation behavior of DCPD-based polymer aerogels can also be controlled by the amount of catalyst added to the precursor solution. Higher concentrations of catalyst affect the gelation time. Since norbornene addition reduces the gelation time, the effect needs to be compensated by higher catalyst concentrations.

To analyze the above mentioned influences of different concentrations of norbornene and catalyst on the uniformity of wet gel layers, 141 µl (translates to a 50 µm film thickness) of a 25 mg/cc p-DCPD/toluene precursor solution with different amounts of norbornene and Grubbs' 1st generation catalyst were filled into different 10 ml glass ampoules and rotated for 20 hours with 11 rotations per minute. To prevent evaporation of the precursor solution during rotation, the ampoules were sealed with a Polytetrafluoroethylene-Copper-sealant tape (figure 4). The rotation speed of 11 rpm and the layer thickness of 50 µm were chosen so that they are as close as possible to the target fabrication process in an ablator shell.

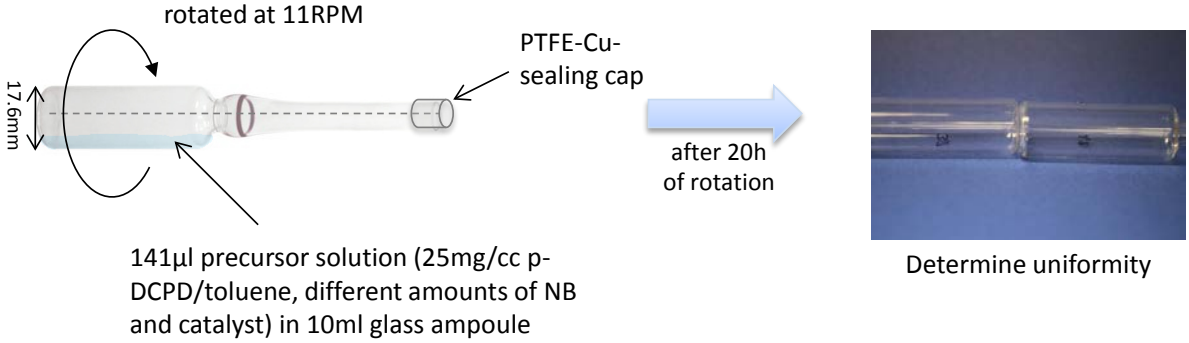

Figure 4: Schematic coating setup: the different 10 ml glass ampoules are filled with 141 µl of the precursor solution, which consists of 25 mg/cc p-DCPD/toluene and different concentrations of norbornene and catalyst. 141 µl equates to a wet gel's layer thickness of 50 µm for the given setup. The glass ampoules with precursor solution were sealed with a PTFE-Cu-sealing tape to prevent evaporation of the solution during rotation. After 20 hours of rotation with 11 rpm the uniformity was determined by optical analysis.

After 20 hours of rotation, which is sufficient time to cure the gel, the uniformity of the wet gel was analyzed optically. An example for different uniformities is shown in figure 5, where 141 µl of a 25 mg/cc DCPD/toluene precursor solution were rotated with 11 rpm for 20 hours. One of them had 0 wt.% NB and 0.2 wt.% catalyst (figure 5a), which leads to a non-uniform wet gel layer with a high number of

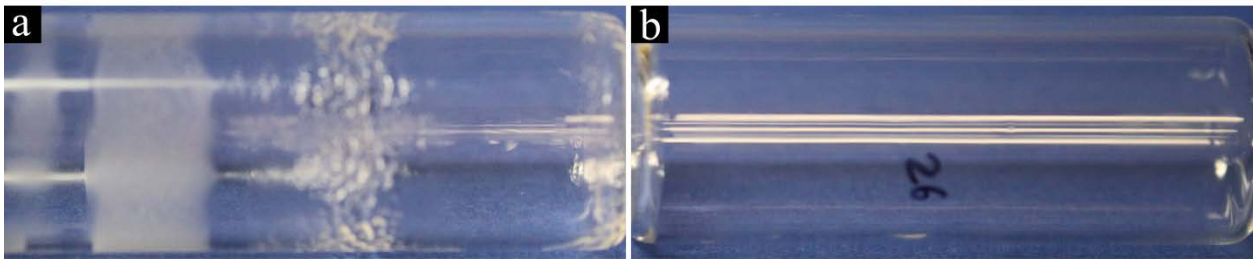

Figure 5: Effects of norbornene (NB) and catalyst addition on gelation of a 25 mg/cc p-DCPD gel in toluene rotated with 11rpm for 20 hours: a) 0 wt.% NB, 0.2 wt.% catalyst; b) 15 wt.% NB, 0.2 wt.% catalyst

irregularities, whereas the same experiment, but this time with 15 wt.% NB with 0.2 wt.% catalyst lead to a uniform wet gel layer. Consequently, the vial shown in figure 5a is rated a low quality wet gel layer (1 on the uniformity scale) and the vial shown in figure 5b as a high quality wet gel layer (5 on the uniformity scale).

This experiment was repeated for different amounts of NB, keeping the catalyst concentration constant as well as changing the concentration of the catalyst with a constant amount of NB. All experiments were conducted twice to ensure reproducibility. A comparison of the results reveals that a higher catalyst concentration leads to less uniform wet gel layers, as seen in figure 6a and figure 6b. More catalyst in the precursor solution results in more, but shorter polymer chains. The shorter chains have less effect on viscosity than few longer ones. In addition to the advantage of a more uniform film, a small amount of catalyst incorporated into the polymer network is preferred as the catalyst has a high atomic number and would, therefore, quench the fusion reaction.

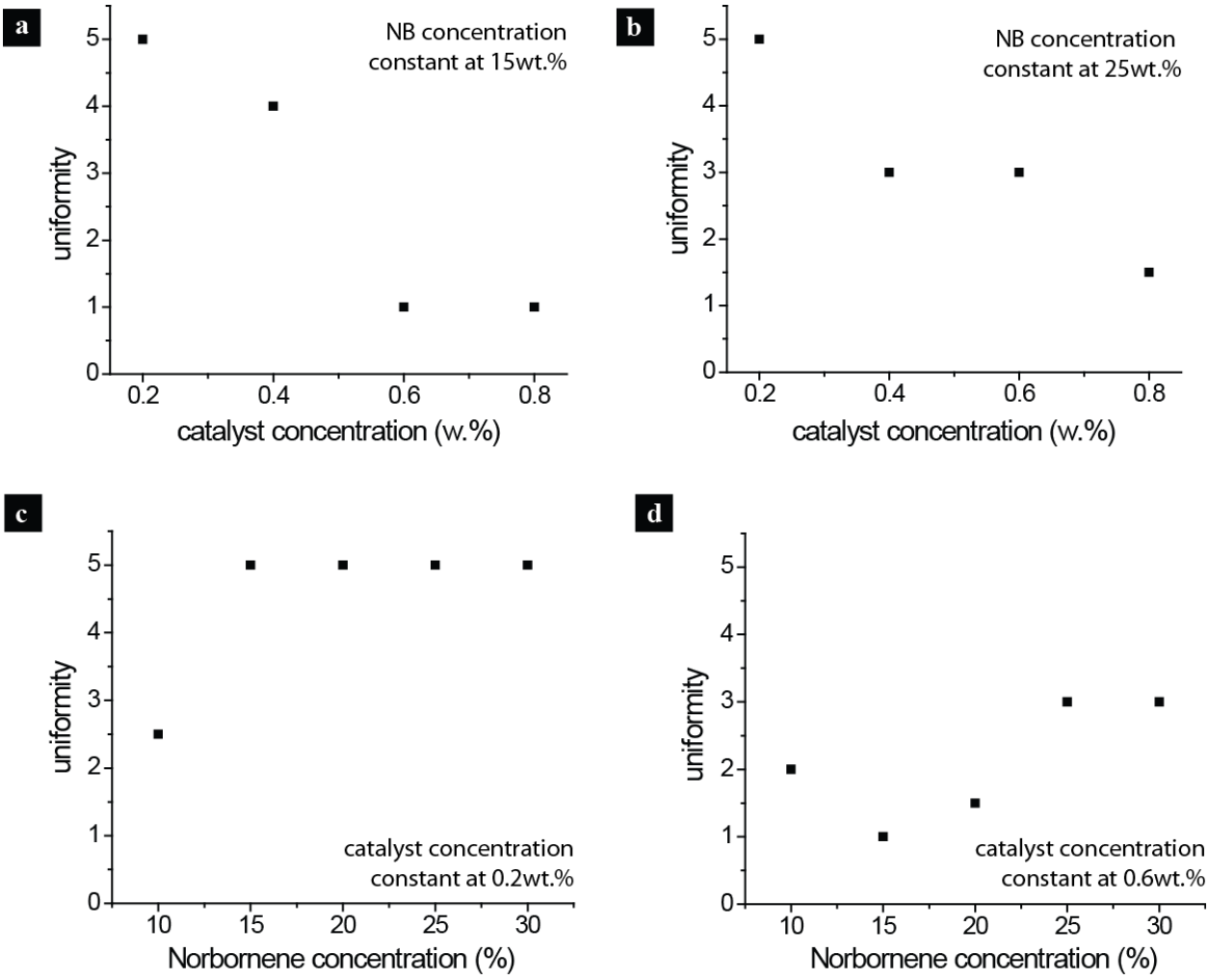

Figure 6: Influence of norbornene and catalyst addition on the uniformity after gelation of a 25 mg/cc p-DCPD gel in toluene: a) 15 wt.% NB with different catalyst concentrations: higher catalyst concentrations lead to less uniform films; b) 25 wt.% NB with different catalyst concentrations: higher catalyst concentrations lead to less uniform films; c) 0.2 wt.% catalyst with different norbornene concentrations; d) 0.6 wt.% catalyst with different NB concentrations.

Increasing the concentration of norbornene on the other hand seems to lead to more uniform films, as seen in figure 6c and figure 6d. This can be explained by the fact, that the addition of NB reduces the amount of cross linking, which increases the viscosity as mentioned in[58]. The elevated gel point viscosity

reduces the shear, which the DCPD experiences during gelation, which can be expressed by the equation derived by F. Melo[59]:

$$\omega = \frac{2.14 g \rho h^2}{R \mu}. \quad (1)$$

The angular velocity ω is inverse proportional to the dynamic viscosity μ and since the shear rate is proportional to the angular velocity, an increase in viscosity at the gel point reduces the shear forces, which the gel experiences during polymerization. Consequently higher NB concentrations lead to more uniform films.

In order to compare the obtained results and finding the desired concentration for upcoming experiments and the target fabrication process, all data acquired were combined into Table 1.

Table 1: Uniformity-dependency of a 25 mg/cc poly-dicyclopentadiene (p-DCPD) gel in toluene to norbornene and catalyst concentrations. "1" represents a low quality wet gel layer with a high number of irregularities and "5" represents a uniform, almost transparent, film layer.

Catalyst conc. [w.%] \ Norbornene conc. [%]	10	15	20	25	30
0.2	2.5	5	5	5	5
0.4	2	4	4	3	4
0.6	2	1	1.5	3	(3)
0.8	3	1	2	1.5	3.5

As mentioned above a small concentration of catalyst and NB, which still leads to a uniform film layer is preferable, which is why a concentration between 15 wt.% and 20 wt.% NB and 0.2 wt.% catalyst for a 25 mg/cc DCPD/toluene wet gel is used during the following experiments.

2.1.2 Film Thickness

The next parameter of interest is the dependency of the wet gel layer thickness to the uniformity of the aerogel. As stated by equation (1) the angular velocity increases with a higher film thickness and therefore results in an elevated shear rate during polymerization. This suggests that a thicker wet gel layer thickness would lead to less uniform films. With the intention of testing this hypothesis 25 mg/cc DCPD/toluene wet gel layers with different thicknesses were coated into 10 ml glass ampoules (figure 7).

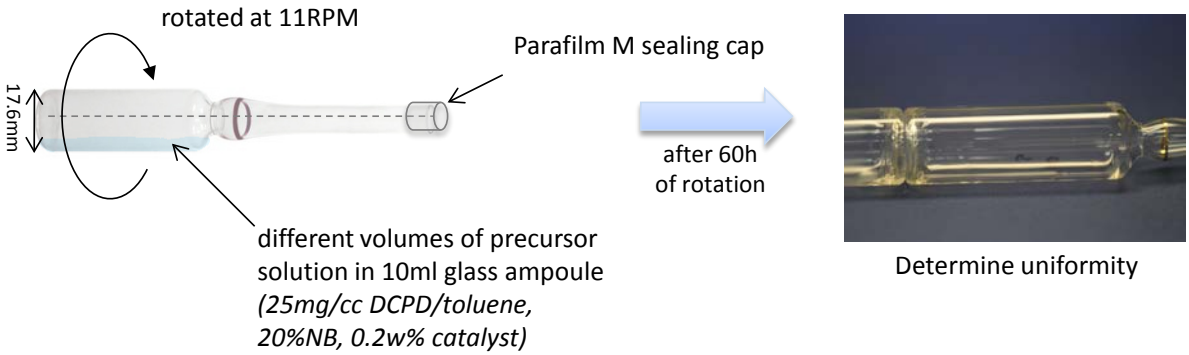

Figure 7: Schematic coating setup: the different 10 ml glass ampoules are filled with different amounts of the precursor solution, which consists of 25 mg/cc p-DCPD/toluene, 20 wt.% norbornene and 0.2 wt.% Grubbs' 1st generation catalyst. The glass ampoules with precursor solution were sealed with a Parafilm M sealing cap to prevent evaporation of the solution during rotation. After 60 hours of rotation with 11 rpm the uniformity was determined by optical analysis.

The norbornene concentration was set to 20 wt.% and the Grubbs' 1st generation catalyst concentration to 0.2 wt.% since they lead to uniform films as determined in the experiment above. The uniformity of the wet gel layer was analyzed after 60 hours of rotation with 11 rpm. As shown in figure 8a), the vials are coated almost uniformly, with the exception that in vials with a thicker film layer, parts of the aerogel seem to form lumps at the end of the vial, while the middle part is coated uniformly. This is due to the wetting behavior of the precursor solution, which drags parts of the solution towards the end of the vial

and allows it to polymerize there. In the target fabrication process this effect is negligible as the targets have a spherical shape opposed to the cylindrical shape used in this experiment.

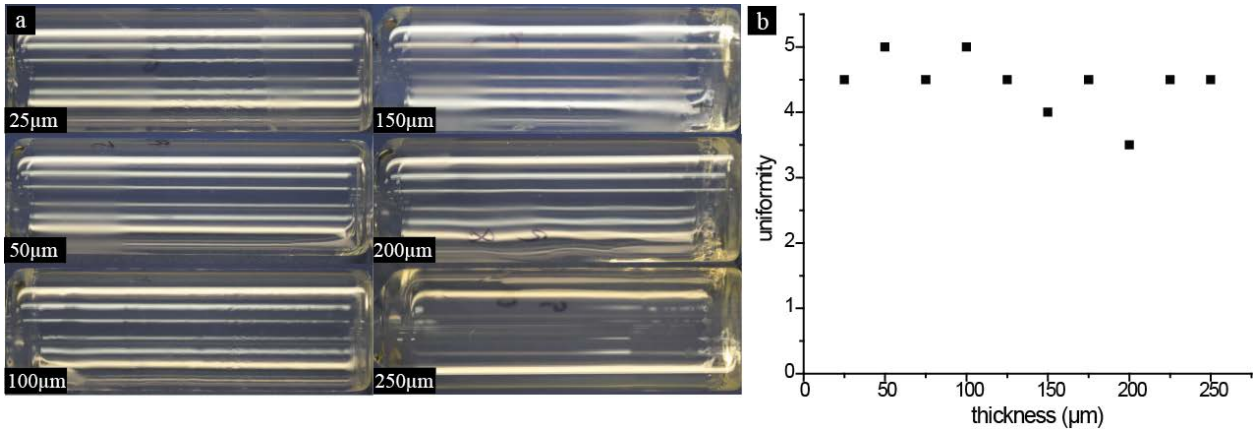

Figure 8: dependency of the wet gel layer thickness to the uniformity of the aerogel: a) different film thicknesses of 25 mg/cc p-DCPD/toluene wet gels coated in glass ampoules. The number of irregularities in the wet gel increases to some extent with the film thickness; b) thicker wet gel layers lead to slightly less uniform films.

The formation of bands[60-62] is visible in almost all vials coated. Band formation does not affect the target fabrication process as it does not occur in the spheres. As for the relation between gel-thickness and uniformity, it seems that thinner films are slightly more uniform, but a clear trend was not visible. Almost all vials were coated uniformly and consequently, for 25 mg/cc p-DCPD/toluene precursor solution with 20 wt.% NB and 0.2 wt.% Grubbs' 1st generation catalyst, different thicknesses of the wet gel layer between 25 µm and 250 µm do not have a severe effect on the uniformity of the film. The repetition of the experiment, however, did lead to inconclusive results. Therefore, the analysis should be repeated to confirm the above mentioned results.

2.1.3 SBS Addition

R.R. Paguio reported how adding a styrene-butadiene-styrene (SBS) block copolymer into the precursor solution of resorcinol formaldehyde foam shells increases its uniformity significantly[37]. SBS block copolymers allow modifying the rheological properties of the precursor solution without reacting with it. Since this improvement was achieved by adding the small amount of 0.6 wt.% of SBS into the solution, which

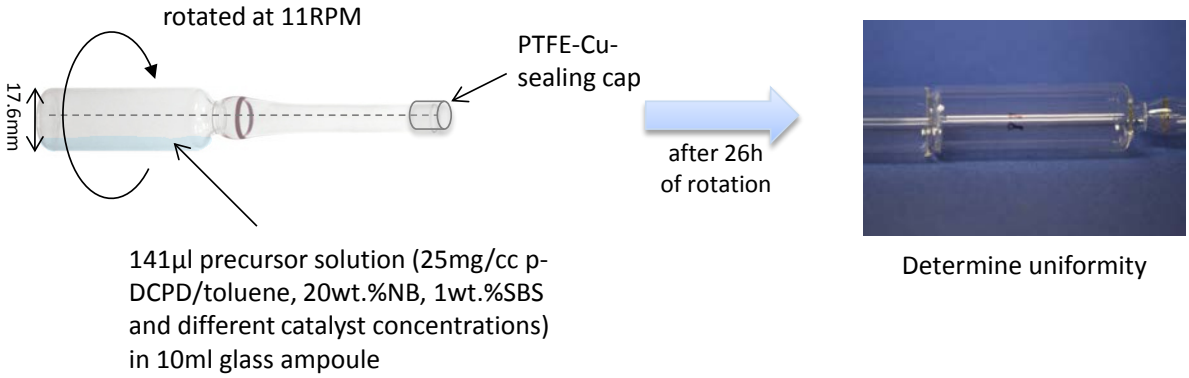

Figure 9: Schematic coating setup: the different 10 ml glass ampoules are filled with 141 µl of the precursor solution, which consists of 25 mg/cc p-DCPD/toluene, 20 wt.% norbornene and different amounts of Grubbs' 1st generation catalyst. The glass ampoules with precursor solution were sealed with a PTFA-copper sealing cap to prevent evaporation of the solution during rotation. After 26 hours of rotation with 11 rpm the uniformity was determined by optical analysis.

resulted in an increase in viscosity, the functionality of this particular block copolymer with the p-DCPD aerogels was tested empirically. For the experiment 1 wt.% of styrene-butadiene-styrene block copolymer was added into different precursor solutions (25 mg/cc p-DCPD/toluene, 20 wt.% NB) with different concentrations of Grubbs' 1st generation catalyst. Different vials with a 50 µm film were coated by rotating the vials containing the precursor solution with 11 rpm for 26 hours. All experiments were repeated at least twice to ensure reproducibility. Figure 10 provides an exemplary selection of the obtained results.

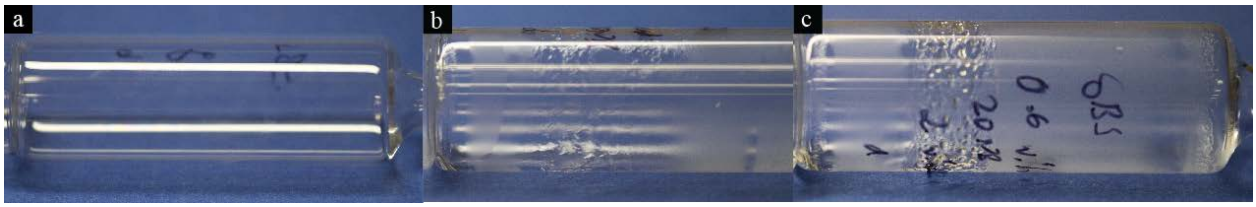

Figure 10: Effects of styrene-butadiene-styrene (SBS) block copolymer addition to the precursor solution on the uniformity of wet gels: 25 mg/cc p-DCPD/toluene, 20 wt.% norbornene, 1 wt.% SBS and a) 0.2 wt.% Grubbs' 1st generation catalyst – no change in uniformity; b) 0.4 wt.% Grubbs' 1st generation catalyst – no change in uniformity; b) 0.6 wt.% Grubbs' 1st generation catalyst – no change in uniformity compared to the control experiment.

The uniformity of the wet aerogel did not improve nor worsen by adding a styrene-butadiene-styrene block copolymer into the precursor solution. The gels had the same uniformity as in the control experiment without the block copolymer. Different concentrations of SBS block copolymer (2 wt.% SBS, 3 wt.% SBS and 10 wt.% SBS) in the precursor solution were tested, but in all cases an improvement in uniformity could not be observed. It seems that the styrene-butadiene-styrene block copolymer does not have an influence on the uniformity of p-DCPD aerogels.

2.1.4 Rotation Delay

The fourth approach to further increase the uniformity of the p-DCPD aerogel after rotation was adding a certain delay time before applying shear forces to the forming polymer network. This delay time would allow the aerogel's network to build up some viscosity and consequently to develop and gain certain strength stationary before the p-DCPD experiences shear forces during gelation, which would lead to a more uniform film. Therefore, 100 µm thick 25 mg/cc p-DCPD layers were coated into different 10 ml glass ampoules with certain different delay times before rotation. The set of experiments was repeated for different amounts of norbornene and Grubbs' 1st generation catalyst and, as usually, all experiments were conducted at least twice to ensure reproducibility of the results. In order to increase the visibility of the wet gels Solvent Blue 35 (17354-14-2) was added to the precursor solution as a dye[63].

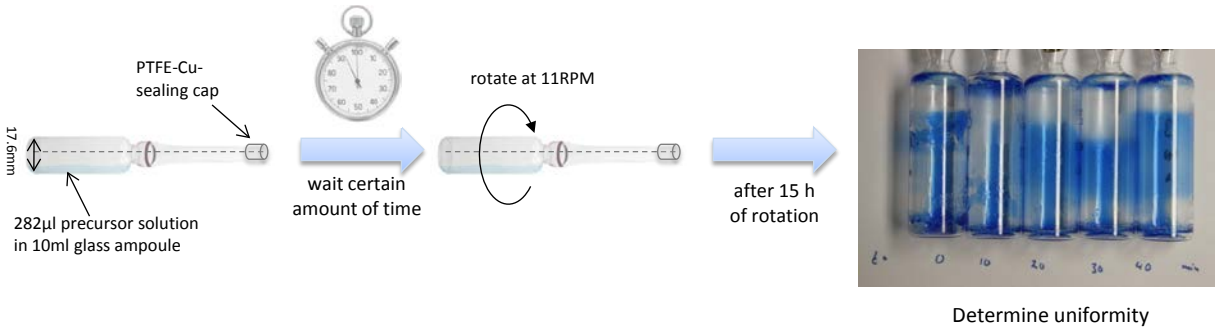

Figure 11: Schematic coating setup: the different 10 ml glass ampoules are filled with 282 µl of the precursor solution, which consists of 25 mg/cc p-DCPD/toluene and different amounts of Grubbs' 1st generation catalyst and norbornene. The glass ampoules with precursor solution were sealed with a PTFA-copper sealing cap to prevent evaporation of the solution during the waiting period and rotation. After a certain amount of time the glass ampoules were rotated for 15 hours with 11 rpm and after rotation the uniformity was determined by optical analysis.

After 15 hours of rotation the uniformity of the wet gel layer was determined optically. Four different sets of precursor compositions were tested: a) 15 wt.% NB, 0.2 wt.% catalyst; b) 15 wt.% NB, 0.4 wt.% catalyst; c) 25 wt.% NB 0.4 wt.% catalyst; d) 25 wt.% NB, 0.6 wt.% catalyst. The results are shown in figure 12.

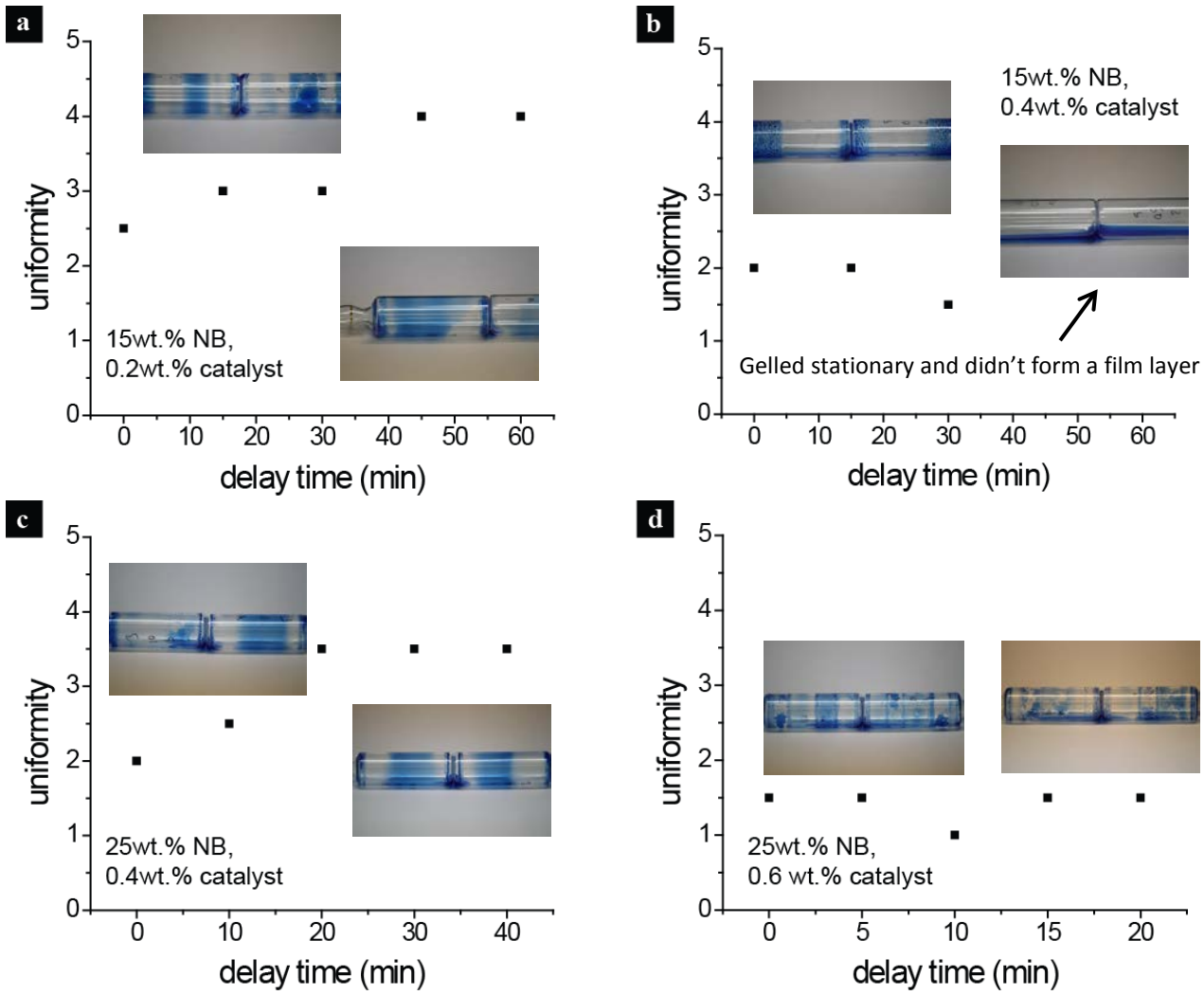

Figure 12: Uniformity-comparison of 100 µm thick 25 mg/cc poly-dicyclopentadiene (p-DCPD) gels in toluene with Solvent Blue 35 as dye and different amounts of Norbornene (NB) and Grubbs 1st-generation catalyst: a) 15 wt.% NB, 0.2 wt.% catalyst; b) 15 wt.% NB, 0.4 wt.% catalyst; c) 25 wt.% NB 0.4 wt.% catalyst; d) 25 wt.% NB, 0.6 wt.% catalyst. Each data point indicates a different vial with a certain delay time before shear forces were applied.

Figure 12a) and c) indicate that a delay time before rotation indeed does increase the uniformity of the wet gel layer. For a 25 mg/cc p-DCPD gel in toluene with a concentration of 15 wt.% norbornene and 0.2 wt.% catalyst a delay in gelation of 45 minutes increases the uniformity significantly, while for a wet gel with 25 wt.% norbornene and 0.4 wt.% catalyst a 20 minute postponed start of rotation is sufficient to enhance its uniformity. A delay time longer than 45 minutes is too long for a wet gel with 15 wt.% NB and 0.4 wt.% catalyst, because the solution already completed the gelation and is, therefore, not able to coat the vial during rotation (figure 12b). The uniformity did not improve for a concentration of 25 wt.% norbornene and 0.6 wt.% catalyst within 20 minutes since the catalyst concentration was too high, which had a higher contribution than the gelation delay on the wet gel's uniformity. Figure 13 illustrates the two sets of experiments, in which a significant change after adding a delay time could be observed.

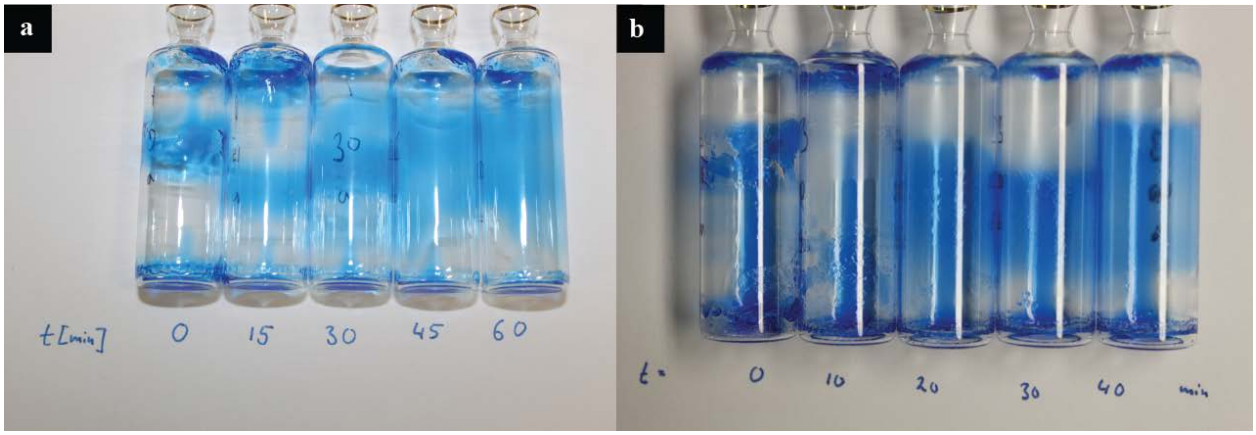

Figure 13: Influence of a gelation delay before rotation on the uniformity for a 25 mg/cc p-DCPD gel in toluene: a) 15 wt.% NB, 0.2 wt.% catalyst; b) 25 wt.% NB, 0.4 wt.% catalyst. The increasing delay time in minutes for each vial is shown below the vial. Solvent Blue 35 was added as a dye to improve the visibility of the gel.

The trend of improvement in uniformity with increasing delay time is clearly visible. As described above the formation of bands during rotation could be easily observed, which are not taken into account for the determination of the uniformity. The control experiment, however, with no delay time before rotation deviated considerably from previous experiments. The uniformity should have been in the same regime and consequently, the experiment was repeated without the dye in order to eliminate the possibility that

the dye (Solvent Blue 35) affected the polymerization and influenced the outcome of the experiment. An additional modification made to the experiment was a decrease of steps in the delay time to get a more accurate measurement and also to prevent stationary gelation as in the previous experiment observed. The results are summarized in figure 14.

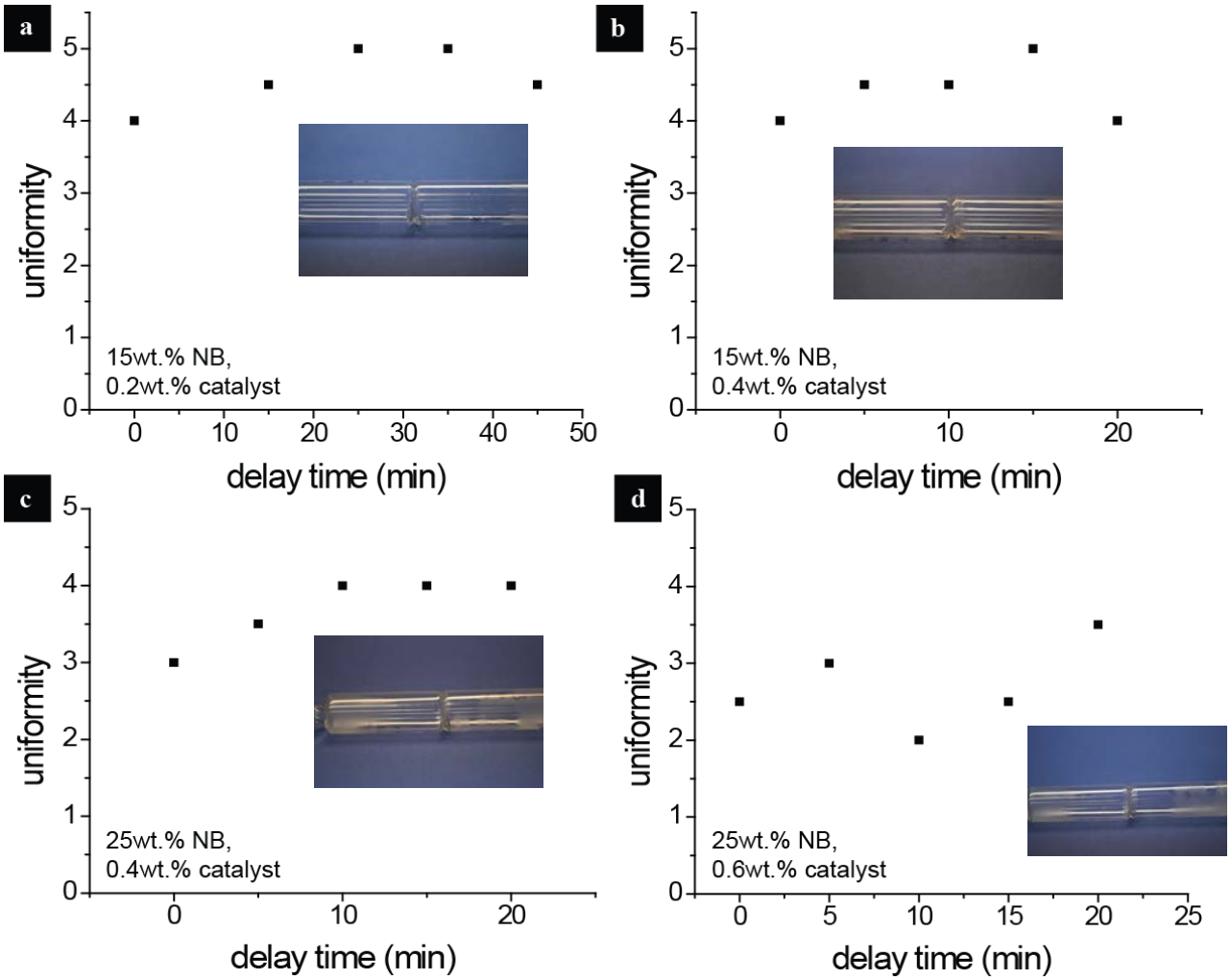

Figure 14: Uniformity-comparison of 50 µm thick 25 mg/cc poly-dicyclopentadiene gels in toluene and different amounts of Norbornene (NB) and Grubbs 1st-generation catalyst: a) 15 wt.% NB, 0.2 wt.% catalyst; b) 15 wt.% NB, 0.4 wt.% catalyst; c) 25 wt.% NB 0.4 wt.% catalyst; d) 25 wt.% NB, 0.6 wt.% catalyst. Each data point indicates a different vial with a certain delay time before shear forces were applied.

Comparing this set of experiments to the previous run, it is apparent that the dye slightly affected the wet gel's uniformity. A delay time of 25 minutes for a concentration of 15 wt.% NB and 0.2 wt.% catalyst (figure 14a) and 15 minutes for a concentration of 15 wt.% NB and 0.4 wt.% catalyst (figure 14b) affected the outcome of the experiment positively. Delaying the rotation by 10 minutes for 25 wt.% NB and 0.4 wt.% catalyst also improves the uniformity. The results for the last set of experiment (figure 14d) are to some extent inconclusive as the wet gel's quality deviates with an increasing delay time. Nevertheless all four experiments show that adding a delay time before rotation slightly increases the uniformity of the wet gel layer inside of the glass ampoule after rotation, which is also illustrated in figure 15.

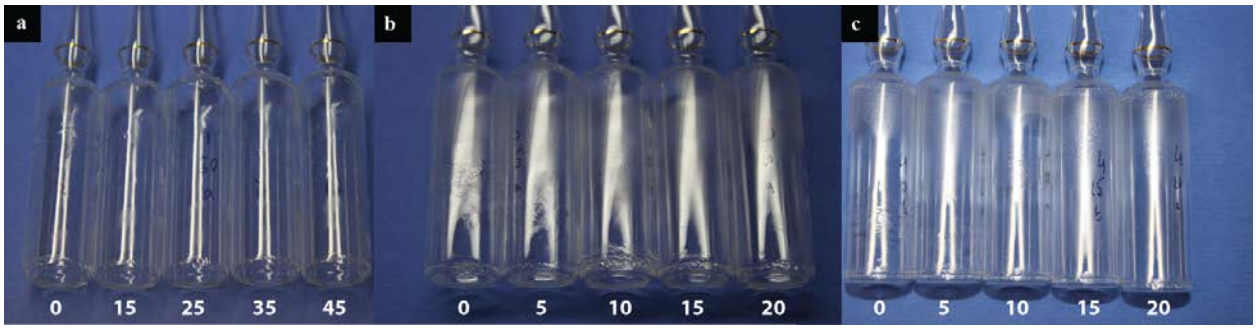

Figure 15: Influence of a gelation delay before rotation on uniformity for a 25 mg/cc p-DCPD gel in toluene: a) 15 wt.% NB, 0.2 wt.% catalyst; b) 25 wt.% NB, 0.4 wt.% catalyst; c) 25 wt.% NB, 0.6 wt.% catalyst. The increasing delay time in minutes for each vial is shown below the vial.

It is noticeable, that the elevated viscosity, which is build up stationary, indeed strengthens the aerogel's network before it experiences shear forces during rotation and, therefore, leads to a more uniform film layer in the glass ampoule.

The delay experiments were repeated in spherical high density carbon ablator shells for the target fabrication process and, unfortunately, did not provide conclusive results, as it was not possible to observe a change in uniformity. This, however, is understandable, since the targets are much smaller and, consequently, do not provide the same opportunity to observe such small differences in the uniformity of

the film layer. While it was possible to determine the wet gel's quality inside the glass ampoules optically, the targets were analyzed with an x-ray source, which does not allow detecting small changes in uniformity. A method to optically analyze spherical high density carbon shells with foam coated inside is currently in development. This would allow validating the above obtained results inside of a target. Nonetheless, the delay experiments were a success as they provided yet another possibility to improve the uniformity of the film layers.

2.1.5 Prepolymerization Experiments

The last approach to increase the uniformity of the p-DCPD aerogel was a two-step prepolymerization[64] experiment, in which the norbornene monomer was prepolymerized first and then, after waiting a certain amount of time, the DCPD was added.

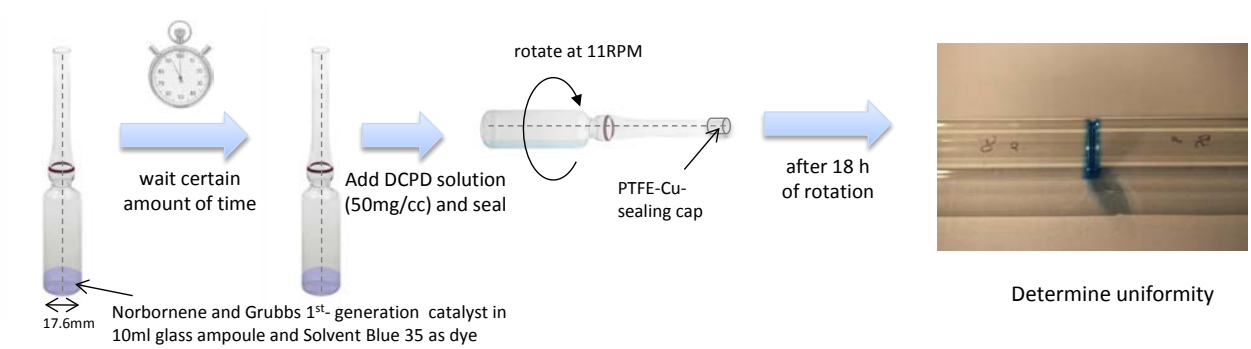

Figure 16: Schematic coating setup: the different 10 ml glass ampoules are filled with norbornene, Grubbs 1st-generation catalyst, and, in one case, Solvent Blue 35 as a dye. After a certain amount of time the 50 mg/cc p-DCPD/toluene solution was added and the vials were sealed with a PTFA-copper sealing cap to prevent evaporation of the solution during rotation. The glass ampoules were rotated for 18 hours with 11 rpm and after rotation the uniformity was determined by optical analysis.

This attempt, as in the previous experiment, would allow building up some viscosity before the entire precursor solution experiences shear forces during rotation. Therefore, the polymer network is strengthened, which would lead to a more uniform film. In a singular set of experiments Solvent Blue 35 was added to the norbornene and catalyst as a dye before adding the DCPD/toluene solution to exemplify what happened during the experiments. All other experiments in this series were conducted without the dye, but lead to the same result. All experiments were conducted at least twice to ensure reproducibility of the results.

Three different time periods before adding the p-DCPD/toluene solution were analyzed: 20, 30, and 40 minutes.

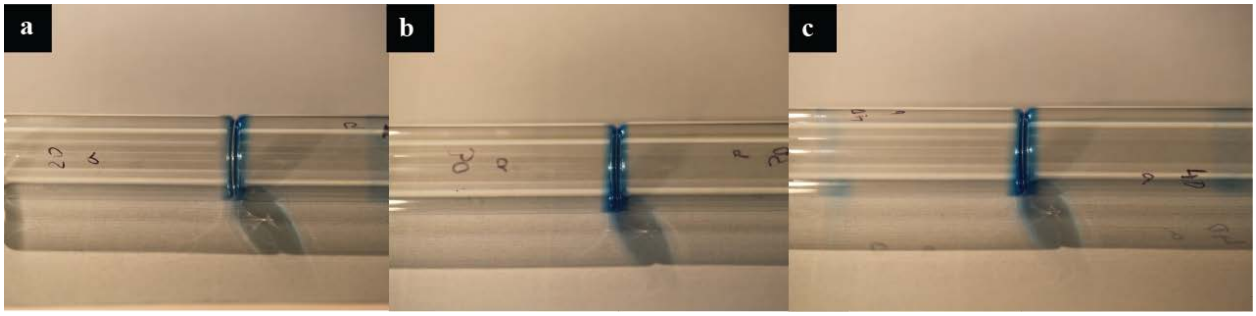

Figure 17: Prepolymerization of a 50 mg/cc poly-dicyclopentadiene gel with 20 wt.% Norbornene and 0.2 wt.% Grubbs 1st generation catalyst in toluene: a) Prepolymerization length: 20minutes; b) Prepolymerization length: 30 minutes; c) Prepolymerization length: 40 minutes.

The polymerization of the norbornene itself took less than 20 minutes, which made it impossible to coat the inside of the glass ampoule with a uniform film after adding the p-DCPD/toluene. The solution gelled before rotation started and the dyed norbornene stayed at the bottom of the vials, which is illustrated in figure 17. As a follow up experiment the prepolymerization time was reduced by a factor of 4, but the same effect was observed. The norbornene gelled almost immediately, which made it impossible to achieve a uniform coating inside of the glass ampoule. In a different approach, small amounts of DCPD/toluene were added to the solution before prepolymerization, but the behavior did not differ compared to the previous experiments. The gelation occurred within a few minutes, which is much faster than the preliminary process for the coating process of the targets. Therefore, prepolymerization with the given values seems to be unsuitable for coating experiments of ICF-targets.

2.1.6 Summary of uniformity experiments

Melo's equation states that an increase in viscosity at the gel point reduces the shear forces, which the gel experiences during polymerization. Various techniques were tested to influence the uniformity of wet p-DCPD aerogel layers to improve the quality of the wet gel.

First the optimal composition of the precursor solution was determined in a systematic study by testing different amounts of norbornene and catalyst concentrations. For a 50 mg/cc p-DCPD/toluene aerogel the optimal composition is 10 wt.%NB and 0.1 wt.% Grubbs 1st-generation catalyst and for a 25 mg/cc p-DCPD/toluene aerogel 15 wt.%NB and 0.2 wt.% catalyst.

It was then tested, whether the uniformity of one specific composition is, as predicted by Melo, influenced by the film thickness of the wet gel layer. For a 25 mg/cc p-DCPD/toluene precursor solution with 20 wt.% NB and 0.2 wt.% catalyst, thicknesses of the wet gel layer between 25 µm and 250 µm were tested, which didn't influence the uniformity of the film.

As reported by R.R. Paguio the addition of styrene-butadiene-styrene (SBS) block copolymer into the precursor solution of resorcinol formaldehyde foam shells increases its uniformity significantly. The functionality of this particular block copolymer with p-DCPD aerogels was tested, but no improvement of the uniformity could be observed.

Delaying the gelation by a certain amount of time strengthens the polymer network before it is exposed to shear and, therefore, influences the uniformity. Different compositions with various delay times were tested, confirming the hypothesis. The effect could not be verified during coating experiments in an ablator shell, but a method to confirm the results is in development.

Prepolymerization of the precursor solution and the resulting increase of its viscosity was found to be unsuitable for the target fabrication process as the reaction occurred too quickly.

The results of these experiments helped facilitating the fabrication process of foam lined ignition targets for inertial confinement fusion experiments. In order to coat an aerogel layer inside of an ablator shell, the precursor solution, however, needs to be precisely injected into the shell.

2.2 Pressure Filling Method

After establishing a suitable formulation for the precursor solution, which allowed coating uniform films, its coating abilities inside of a potential ICF target were tested. This required developing a method, which allows reproducibly injecting 0.1-1 µl of the precursor solution into the ablator. For 2 mm diameter shells, this translates into a film layer thickness of 10-130 µm. As an ablator material high density carbon shells[65] were used, which are hollow diamond spheres with 2 mm inner diameter and a wall thickness of approximately 30 µm. Each sphere has a hole drilled into it with an inner diameter of 30-50 µm through which the precursor solution can be inserted. The custom built filling setup is described in detail in figure 18a. It consists of a small vacuum chamber that contains a vial filled with the precursor solution and a linear feedthrough to which the ablator shell is attached.

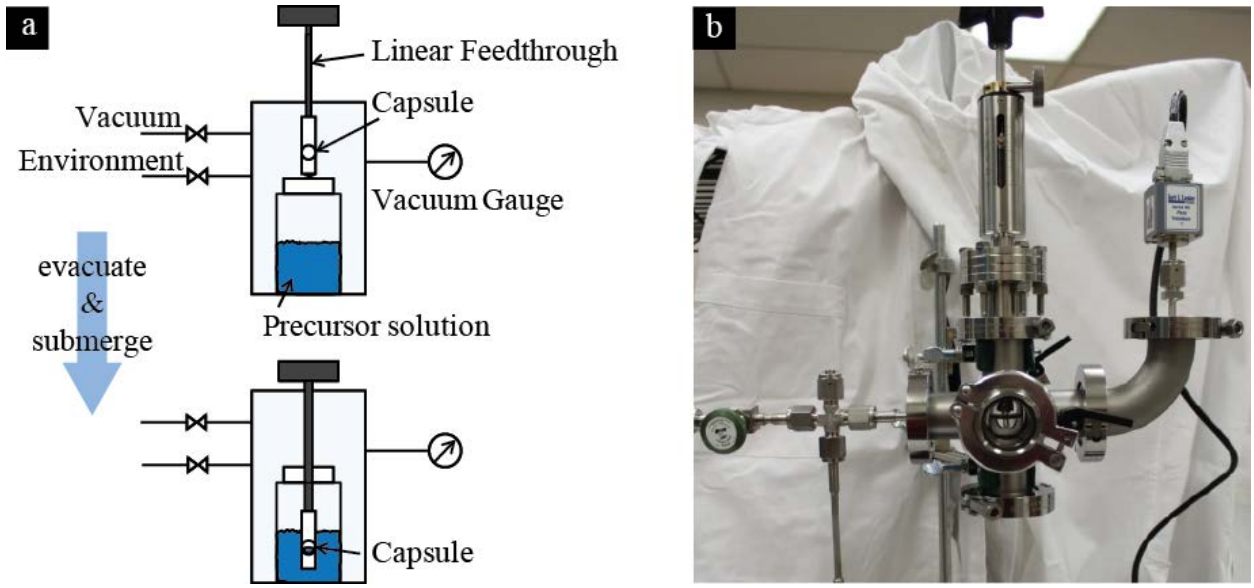

Figure 18: Capsule filling setup and filling calibration: (a) the filling setup consists of a small vacuum chamber that contains a vial with the aerogel precursor solution and a linear feedthrough to which the ablator shell is attached. To achieve high reproducibility with high accuracy, it is crucial to underpressurize the capsule before submerging it into the precursor solution; (b) picture of the developed setup during the experiment: the ablator shell can be seen through the viewport of the experiment.

First, the chamber is slightly underpressurized (20-250 torr below atmospheric pressure, depending on the desired foam layer thickness) while the capsule is not in contact with the precursor solution. This prevents the formation of air-bubbles attached to the fill hole that is critical for achieving the required reproducibility. The under-pressurized capsule is then submerged in the precursor solution, and filled by re-pressurizing the chamber to atmospheric pressure.

It is essential that the film layer thickness inside of the ablator shell can be controlled reproducibly on a µm-scale. For that reason, the dependency of injected volume to applied pressure differential was analyzed and compared to the ideal gas law

$$\Delta V = (V_s/p_o)\Delta p,$$

where ΔV is the injected volume, Δp is the applied pressure differential, and V_s and p_o are the shell volume (4.2 µl) and standard pressure (760 torr), respectively. The injected volume was acquired by weight gain measurements with the density of toluene under ambient conditions (0.867g/cc). Twelve different pressure differentials in the range of 20 to 250 torr were measured. Each of those data points was measured five times to confirm reproducibility. As shown in figure 19, the injected volume and, consequently, the film layer thickness increases, as expected, linearly with the applied pressure differential (with ~0.01 µl precision). The experiment was conducted for two different hole sizes to exclude the possibility of a hole diameter's dependency.

The injected volume is almost independent of the hole diameter.

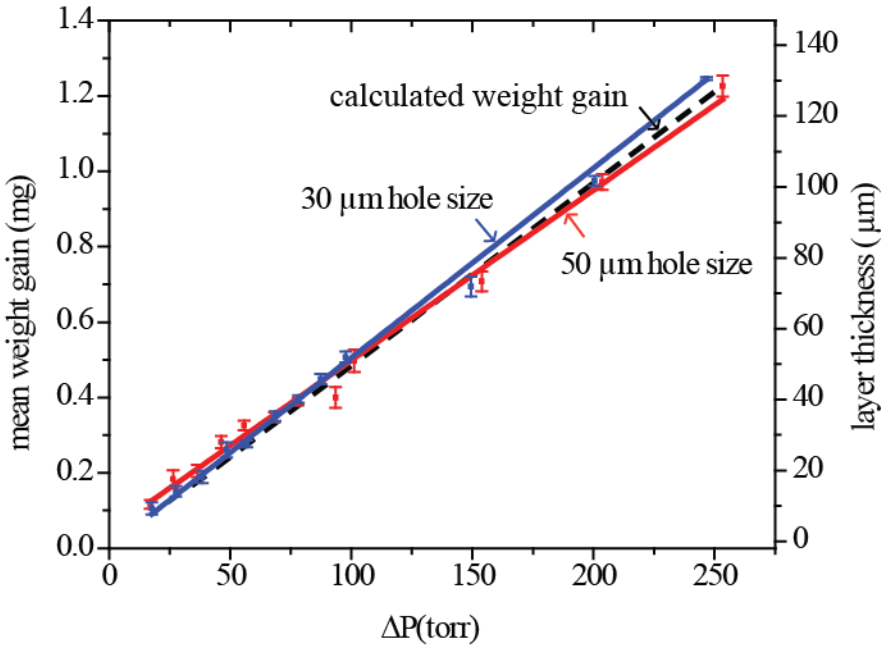

Figure 19: Injected liquid and corresponding layer thickness versus applied pressure differential. The injected volume, as derived from weight gain measurements, follows the linear behavior (dashed line) expected from the ideal gas law and is almost independent of the hole diameter.

This measurement allowed to create a filling standard for high density carbon ablators with a 2 mm diameter. The required pressure differentials, which are required to acquire a certain film layer thickness were extrapolated and summarized in Table 2.

Table 2: Dependency of pressure differential and layer thicknesses inside a 2 mm diamond capsule based on 30 µm sized hole

Pressure difference [Torr]	weight gain [mg]	layer thickness [um]	Pressure difference [Torr]	weight gain [mg]	layer thickness [um]
0	0	0	85	0.42952	41.0885806
5	0.02712	2.495427316	90	0.45467	43.60563458
10	0.05227	4.820797248	95	0.47982	46.1360076
15	0.07742	7.157085342	100	0.50497	48.67987727
20	0.10257	9.504420666	105	0.53012	51.23742502
25	0.12772	11.86293475	110	0.55527	53.8088362
30	0.15287	14.23276164	115	0.58042	56.39430023
35	0.17802	16.61403797	120	0.60557	58.9940107
40	0.20317	19.00690306	125	0.63072	61.60816549
45	0.22832	21.41149893	130	0.65587	64.23696693
50	0.25347	23.82797041	135	0.68102	66.88062192
55	0.27862	26.25646524	140	0.70617	69.53934206
60	0.30377	28.69713409	145	0.73132	72.21334384
65	0.32892	31.1501307	150	0.75647	74.90284875
70	0.35407	33.61561191	200	1.00797	102.7032342
75	0.37922	36.09373781	250	1.25947	132.3420652
80	0.40437	38.58467178			

The results were confirmed by filling a high density carbon ablator shell with a 50 mg/cc DCPD/toluene precursor solution (20 wt.% NB and 0.2 wt.% Grubbs 1st-generation catalyst) with a pressure differential of ΔP=102.4 torr, which was rotated[2] and analyzed afterwards.

[2] The rotation for a spherical target differs from the cylindrical geometry rotation. The process on fabrication of aerogel-lined Indirect-Drive NIF Ignition Targets can be found in [J. Biener *et al* 2012 *Nucl. Fusion* **52** 062001].

As shown in figure 20, the wet gel layer thickness is completely consistent with the previous found dependency between the pressure differential and layer thickness, which allows using this method as a filling standard for the fabrication of aerogel-lined Indirect-Drive NIF Ignition Targets[45].

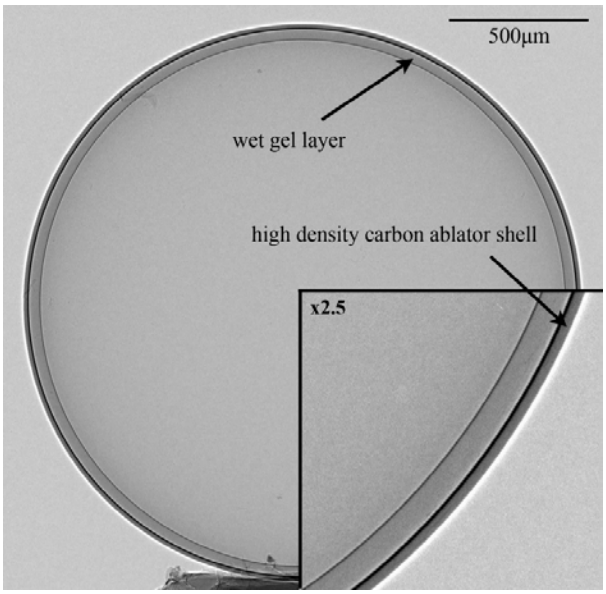

Figure 20: Radiograph of a 2 mm diamond capsule (I.D.) coated with a P(DCPD-r-NB) wet gel layer (50 mg/cc DCPD, 20 wt.% NB, 0.2 wt.% "Grubbs 1"-catalyst, filled at ΔP=102.4 torr, rotated at 10/14.142 rpm for ~5 h)

2.3 USAXS Analysis of Wetting Behavior

After coating thin films with the required thickness into the inside of high density carbon ablator shells, the wet gel layers were typically supercritically dried, typically by direct solvent exchange with carbon dioxide. The gel-coated ablator shells underwent solvent exchange in liquid CO2 at 12°C and 900 psi in a Polaron critical point dryer to replace the toluene in the gel pores with liquid CO2. Once the toluene was exchanged (expected after 10 days), the temperature and pressure in the critical point dryer was increased to the supercritical regime (~50°C and 1600 psi). The pressure was then allowed to slowly decrease to atmospheric pressure while keeping the temperature constant. This leads to ultra-low density foam layers, which can serve as a scaffold to define the shape of the deuterium-tritium fuel layer inside of the ablator and also enable the possibility of introducing dopants directly into the fuel for diagnostics. Therefore it is critical that the aerogel survives the wetting and freezing with liquid deuterium and tritium and does maintain its structural characteristics as liquid induced deformation of the low density porous material could be an issue.[66-68] Because of the foam's ultra-low density, the ability to withstand the wetting is not trivial and needed to be tested and analyzed. The initial wetting experiments for this analysis were performed with hydrogen instead of deuterium and tritium, because it was easier accessible and less complicated to handle. The physical properties are very similar, except the triple point temperature and the beta layering effect due to Tritium's radioactivity. Therefore, the substitution is feasible.

2.3.1 Preliminary Wetting Analysis of Bulk Material

The first experiment conducted was an optical analysis of the wetting behavior of a bulk piece of 25 mg/cc p-DCPD aerogel and its ability to withstand wetting with liquid hydrogen. In order to expose the

aerogel to liquid hydrogen, the sample was placed in a cryostat to achieve the required temperatures to liquefy the hydrogen. After evacuating, hydrogen gas was inserted into the chamber, where the aerogel was placed and cooled down to 15K, which allowed the hydrogen to liquefy. Figure 21 illustrates the process of immersing the 25 mg/cc p-DCPD aerogel into liquid hydrogen, freezing it, and the removal of the hydrogen.

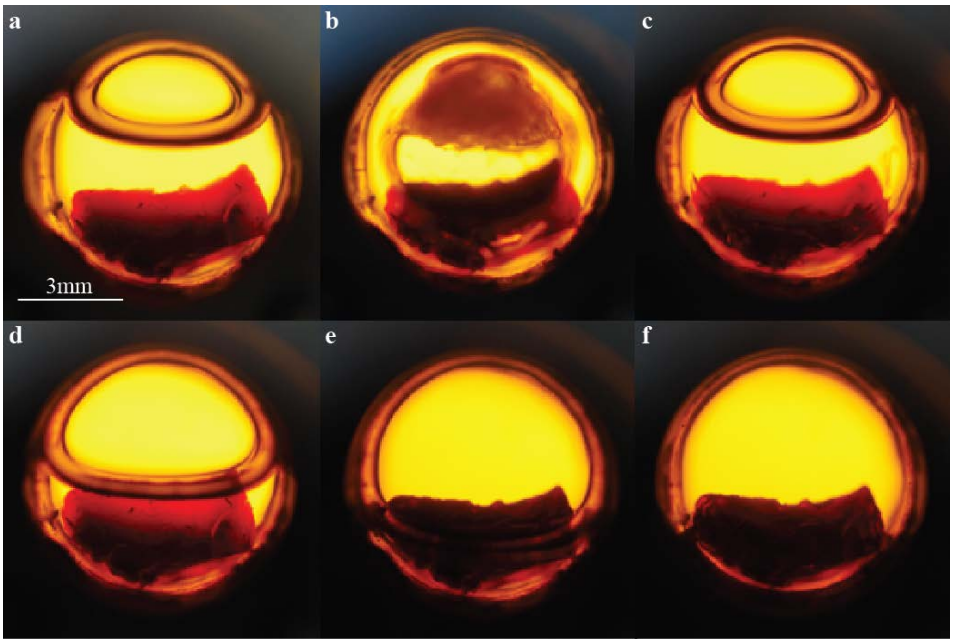

Figure 21: Wetting and freezing of a 25 mg/cc p-DCPD (15 wt.% NB, 0.2 wt.% "Grubbs 1"-catalyst) aerogel in liquid hydrogen: aerogel immersed in (a) liquid and (b) frozen hydrogen. The aerogel keeps its integrity during the wetting as well as during (c)-(e) removing the liquid hydrogen; (f) the dry aerogel can be wetted or frozen again.

DCPD has a higher density (roughly 1g/cc) than liquid hydrogen (roughly 70mg/cc[69]), while the density of the aerogel is just 25mg/cc. It is clearly visible in figure 21a that the aerogel is completely immersed in the liquid hydrogen and does not float, which is a good indicator that its pores are completely filled with liquid hydrogen. After further cooling the hydrogen to 13.6 K the aerogel is immersed in frozen hydrogen (figure 21b). The optical analysis reveals that after increasing the temperature (figure 21c-e) and removing the hydrogen from the chamber, the aerogel kept its structural integrity during the process and did not collapse or fall apart (figure 21f). The wetting and freezing was

done multiple times without any change in results. This experiment serves as a first indicator of the aerogel's ability to withstand wetting and freezing with hydrogen. It does not, however, give any conclusions about potential structural changes on a smaller length scale or on the wetting behavior.

2.3.2 USAXS analysis

In order to detect potential structural changes of the foam with a broad range of resolution on the length scale, the aerogel was analyzed with Ultra Small Angle X-ray Scattering (USAXS)[70, 71]. Typical Small Angle X-ray Scattering experiments allow obtaining information on length scales between 1 and 100 nm[71]. Bragg's law $n\lambda = 2d\sin(\theta)$ states that larger structures have smaller scattering angles and, therefore, to resolve structures with larger dimensions than 100 nm, Ultra Small Angle X-ray Scattering is a practicable method. Since it is a non-destructive measurement technique, it is possible to perform different experiments on the same piece of foam, hence, increasing the accuracy of the measurement. The measurement principle is described in figure 22 and 23.

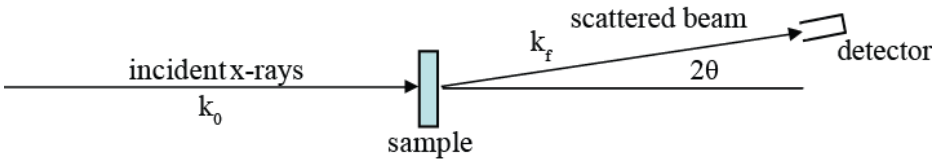

Figure 22: Schematic X-ray scattering: the incident wave vector k_0 is scattered in the sample, resulting in a scattered wave vector k_f, which can be measured by a detector.

The incident x-rays in the experiment are scattered when they hit the sample and by measuring the intensity of the scattered beam at different scattering angles 2θ, the sample can be probed.

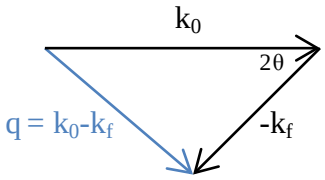

Figure 23: The wave vector transfer, or scattering vector, q can be defined as $q=k_0-k_f$. With $k = \frac{2\pi}{\lambda}$, q can be written as $q = \frac{4\pi}{\lambda}\sin(\theta)$.

Defining a scattering vector $\vec{q}$, where $q = \frac{4\pi}{\lambda}\sin(\theta)$ is its modulus, λ is the wavelength of the X-ray beam and 2θ is the scattering angle, allows expressing the scattered wave from every point of the probed sample as $e^{-i\vec{q}\vec{r}}$. The vector $\vec{r}$ is the position of the respective point in the sample, so that adding up all waves leads to the full scattering amplitude. The intensity is the absolute square of the scattering amplitude. One thing to note is that the intensity for this experiment is expressed in units of [cm^{-1}]. This is due to the fact that the photons scattered into the solid angle $d\Omega$ are normalized to the transmitted photons through the sample in order to measure the differential scattering cross section per unit scattering volume, hence $\frac{\text{detected photons/solid angle}}{\text{area·length·incident photons/area}} = \text{cross section/unit sample volume/unit solid angle} = \frac{d\sigma}{d\Omega \cdot V}[cm^{-1}]$[71, 72]. All USAXS experiments were conducted at beamline 15ID of the Advanced Photon Source (APS) at Argonne National Laboratory and the spectra were acquired by Tony van Buuren and Trevor M. Willey, Lawrence Livermore National Laboratory. The specific design of this particular USAXS instrument at the beamline is described in great detail by J. Ilavsky et al.[71]. For the measurement the samples were placed in a cryostat with liquid helium as a cryogen to reach the preferred temperatures and pressures. The samples were not directly exposed to the helium, but held in vacuum or, if desired, exposed to hydrogen. The acquired data was reduced using the software package *Indra 2* (Ilavsky & Jemian, 2009), a USAXS data reduction macro for IgorPro (Wavemetrics), and for the final analysis of the reduced data, the tool suite for modeling and analysis of Small Angle Scattering *Irena*[73] was used[70].

2.3.2.1 USAXS analysis of free standing foam

For this particular USAXS measurement a free standing cylindrical piece of 30 mg/cc p-DCPD aerogel, with a thickness of 0.25cm and a height of 0.5cm was used. The beam was shot through the entire thickness of the sample. For the initial experiment the aerogel was scanned at ambient conditions and, after reducing and analyzing the data a scattering profile was obtained (figure 24a – 'RT-Atm'). In order to detect potential structural changes during evacuation, the same sample was measured again, this time at room temperature and a pressure of P=0.1 torr, which lead to a second scattering profile (figure 24a – 'RT-Vac'). As figure 24a illustrates, both scattering profiles look exactly alike, which means, there are no structural changes on a length scale between 1nm and 1 µm in the p-DCPD foam during evacuation.

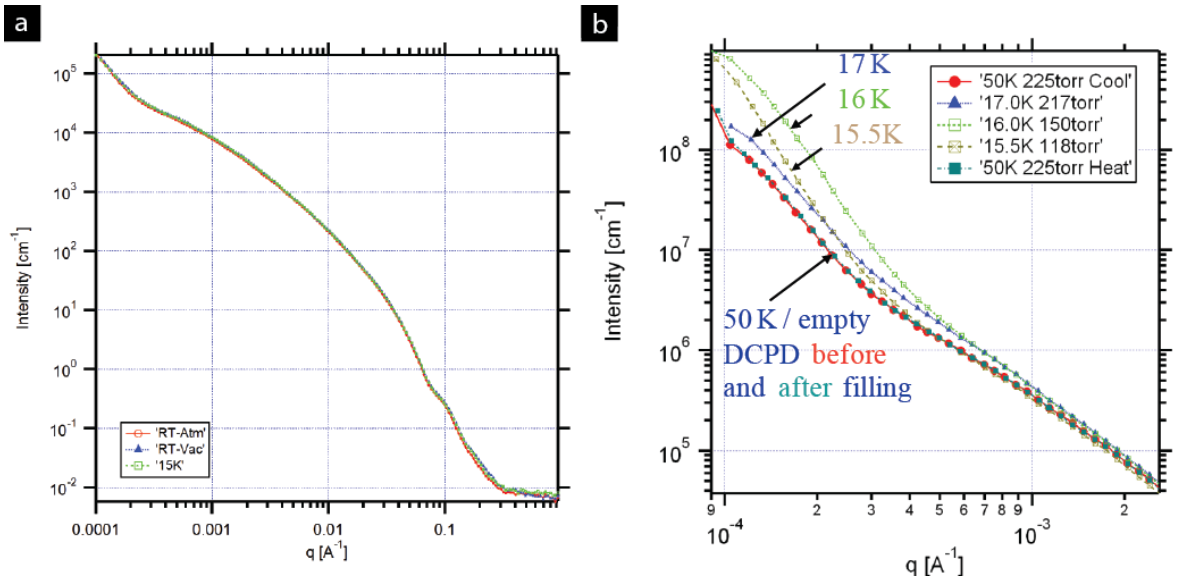

Figure 24: USAXS spectra of aerogels: (a) comparison of a 30 mg/cc p-DCPD carbon aerogel at T=293.15 K and P=743 torr (red), T=293.15 K and P=0.1 torr (blue) and at T=15 K and P=0.1 torr (green). No changes are observed in scattering while cooling the aerogel; (b) USAXS experiments of in situ hydrogen wetting. The scattering in the low q region increases as the temperature decreases and the hydrogen condensates and partially fills the pores. The stability of the 30 mg/cc p-

DCPD aerogel during hydrogen wetting is confirmed by small angle x-ray scattering as the scattering curve before and after filling are the same.

In an additional experiment, the aerogel's ability to keep its structural characteristics at very small temperatures was tested. The small temperatures are required to liquefy hydrogen. The foam was therefore measured again at T=15 K and a pressure of P=0.1 torr (figure 24a – '15K') and, as can be seen, no changes in scattering are observed. This USAXS analysis demonstrates that a freestanding 30 mg/cc p-DCPD aerogel is mechanically robust and maintains its structural integrity at low pressures and low temperatures. The same piece of foam was now exposed to liquid hydrogen. For that, the temperature was brought down to T=50K, the pressure to P=225 torr and the chamber containing the foam was filled with hydrogen gas. The temperature was then brought down further, so that the hydrogen could condensate. Figure 24b shows an increase in scattering during the condensation of the hydrogen. This is due to the fact that the hydrogen starts to partially fill the pores, which provides new scattering interfaces, mainly the liquid-gasiform hydrogen interface. As the sample was further cooled to T=15.5K, more hydrogen condensed, so that the pores were now filled completely with liquid hydrogen. Consequently the scattering intensity decreased, as the liquid-gasiform hydrogen interface disappeared, which can be observed in figure 24b. As a next step, the p-DCPD foam was heated to a temperature of T=50 K and brought the pressure back to P=225 torr, which were the initial conditions of the experiment. This allowed the hydrogen to evaporate, leaving the foam in its original condition. The USAXS scan, which was taken at this particular temperature and pressure after the wetting process shows the exact same scattering profile as it did before the wetting. This means that there were no changes in the foam's structure on the measured length scale and that the structural integrity was kept during the wetting with liquid hydrogen. The experiment was repeated multiple times, to ensure reproducibility and showed the same result. The Small Angle X-ray Scattering experiments confirmed the stability of the 30 mg/cc aerogel during hydrogen wetting, leading to the conclusion that the p-DCPD foam is a suitable candidate for scaffolding the fuel inside of an ICF target.

2.3.2.2 *USAXS analysis of foam in an ICF ablator shell*

The structural stability of free standing p-DCPD foam during hydrogen wetting was confirmed by the USAXS analysis. The free standing piece, however, has a significantly larger volume in comparison to the aerogel inside of an ICF target and was not cured in a confined space. This could potentially lead to structural differences of the foam, which could influence its ability to withstand hydrogen wetting. Therefore, the structure of an aerogel, which was cured inside of an ICF target, needs to be compared to the structure of a free standing piece of aerogel. Ultra Small Angle X-Ray Scattering with its ability to analyze structural differences in a broad range of resolution on the length scale is an extremely suitable technique for this comparison. However, analyzing a 30 mg/cc DCPD aerogel inside of an ICF target is not trivial, as the material of the target shell is high density carbon with a density of roughly 3.5g/cc. The polymer foam inside of the target shell has only a density of 30 mg/cc, which is significantly smaller than the shell density.

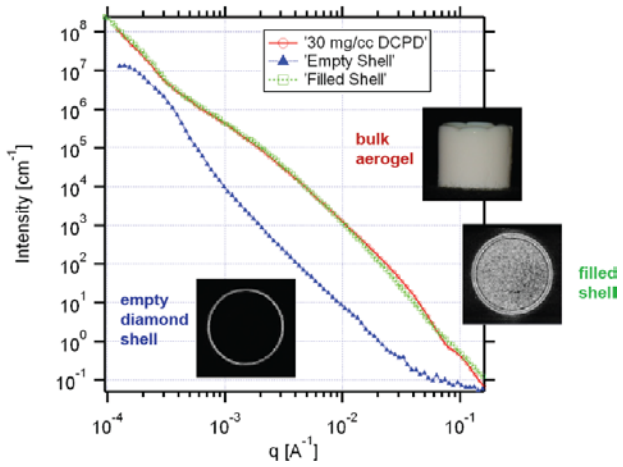

Figure 25: Comparison of USAXS spectra of a free standing p-DCPD foam (30 mg/cc DCPD, 0.2 wt.% "Grubbs 1"-catalyst) with a p-DCPD foam of same composition cured inside of a 2 mm high density carbon shell. The aerogel inside of

the HDC shell and the free standing piece of foam have the same USAXS spectrum and, therefore, the same structure on the measured length scale.

Therefore, a spectrum of an empty diamond shell was acquired, which can be used to normalize against the spectrum of the filled shell, so that the final spectrum only contains the information about the foam inside of the shell. The results are shown in figure 25.

During the next step of the experiment a completely filled ablator shell containing a 30 mg/cc p-DCPD polymer foam was measured and normalized to the empty diamond shell spectrum. This allows analyzing only the foam inside of the shell and comparing it to the free standing piece of the same material. As figure 25 illustrates the DCPD aerogel, which was prepared inside of a target shell has the same spectrum as the freestanding DCPD aerogel, and therefore the same structure on the measured length scales.

Therefore, this experiment serves as a first indicator for the ability of an aerogel cured inside of a target shell to also withstand wetting with hydrogen. Future experiments have to show that the structural integrity is kept during the wetting process and that the results are reproducible for a thin foam layer. The setup, which was used for this particular experiment did not allow acquiring these information and needs to be modified for this purpose. Therefore, an optical analysis of the wetting behavior of liquid deuterium in a thin, dried aerogel film inside of a target shell was completed for this thesis (chapter 2.4, p. 45).

2.4 Deuterium wetting of aerogel inside of an ICF target

The mechanical stability of ultra-low density p-DCPD aerogel bulk pieces during wetting and freezing with liquid hydrogen has been confirmed by optical analysis and Ultra Small Angle X-ray Scattering experiments. In an ICF target, however, the foam is distributed in a thin, uniform layer, which could possibly influence the ability to maintain its structural characteristics. Therefore, an experiment, which allows testing the wetting behavior of thin polymer foam layers, was developed[3]. Since NIF utilizes deuterium and tritium in its experiments and due to better availability, deuterium was used for this experiment. The setup contains of a cryostat with liquid helium as a cryogen to which the high density carbon ablator shell with the dried p-DCPD foam layer is mounted via a fill tube (figure 26a).

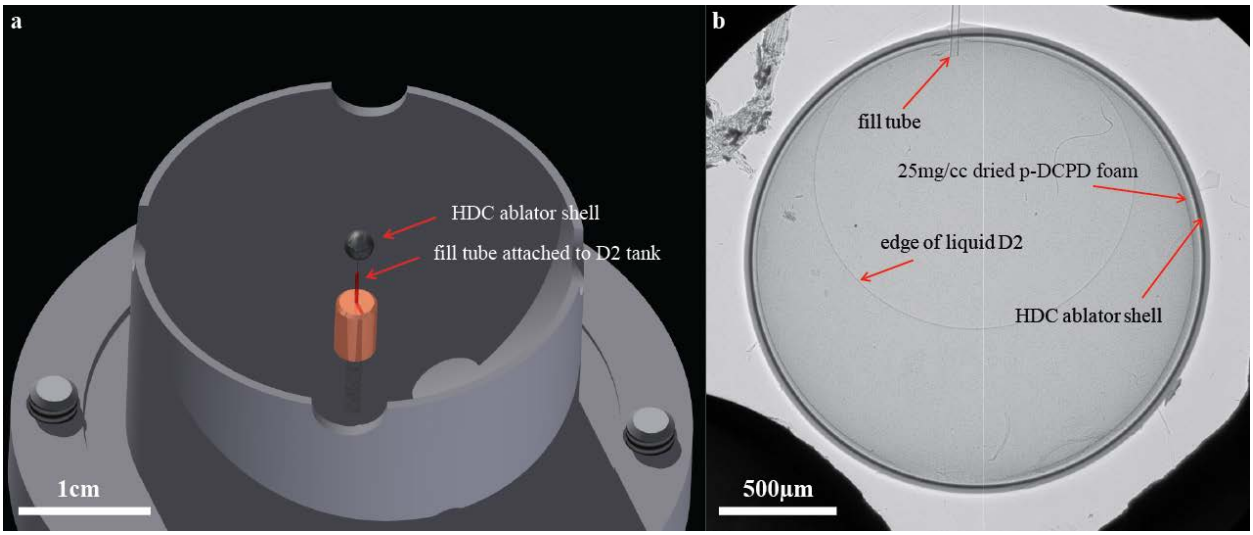

Figure 26: Deuterium filling setup: (a) the high density carbon (HDC) ablator shell with the dried p-DCPD foam is mounted to the cryostat via a fill tube, which itself is attached to a separate deuterium tank. The entire setup is mounted with the fill tube pointing up. For illustration purposes it is shown in a 180° angle; (b) radiograph of the HDC ablator shell coated with dried 25 mg/cc p-DCPD foam and filled with liquid deuterium.

[3] In cooperation with Kuang Jen Wu and Bernard Kozioziemski, LLNL.

The fill tube itself is attached to a separate deuterium tank, which allows controlling the pressure and, therefore, the amount of deuterium inside of the capsule. The temperature is controlled by the liquid helium, which allows cooling the capsule below the condensation temperature of deuterium[74]. The cryostat has two beryllium windows, which allows the ultra-low density p-DCPD foam inside of the HDC shell to be analyzed with an X-ray imaging system[75, 76].

The imaging system consists of a micro-focus X-ray source and a direct-detection X-ray CCD camera. The X-ray source is a Thermo-Kevex PXS927-EA-LV. It has a tungsten anode and is operated at 50kV and 80 µA, so that the X-ray spectrum is peaked between 9 and 11keV, the tungsten L-shell lines. The X-ray spot size is 5 µm for these operating conditions. The CCD camera is a Princeton Instruments PI-LCX 1300 deep depletion layer CCD. The X-rays are converted directly into electrons by the silicon CCD element without any phosphor screen. The X-ray source is placed approximately 100 mm from the HDC shell and the detector is approximately 685 mm from the shell. This large separation between the source and CCD provides both geometric magnification as well as in-line phase-contrast enhanced imaging.[76, 77] The deuterium only weakly absorbs the X-rays with significant transmission through the beryllium windows and the high density carbon shell. However, the refraction, as the X-rays pass nearly tangent to the deuterium solid-vapor or liquid-vapor interfaces, provides sufficient contrast to locate the interface. This imaging setup allows an *in situ* analysis of the deuterium wetting of the foam and also provides information on how the deuterium is distributed inside of the ablator shell. The possibilities include an initial wetting close to the fill tube where the deuterium is inserted, wetting close to the bottom of the shell, or a uniform distribution. The cryostat allows cooling the capsule to perform the foam layering with liquid deuterium, which is done at 19.5K[78, 79].

The foam used during this experiment is a 50 mg/cc p-DCPD aerogel with 10% norbornene and 0.1w.% Grubbs' 1st generation catalyst, which is supercritically dried by direct solvent exchange with carbon dioxide. It was exposed to iodine vapor for 72hours to increase its visibility during radiography in the dry phase (figure 27a).

As illustrated in figure 27 the deuterium wets the dried p-DCPD foam layer uniformly (figure 27b) and the foam maintains its structural integrity during the process.

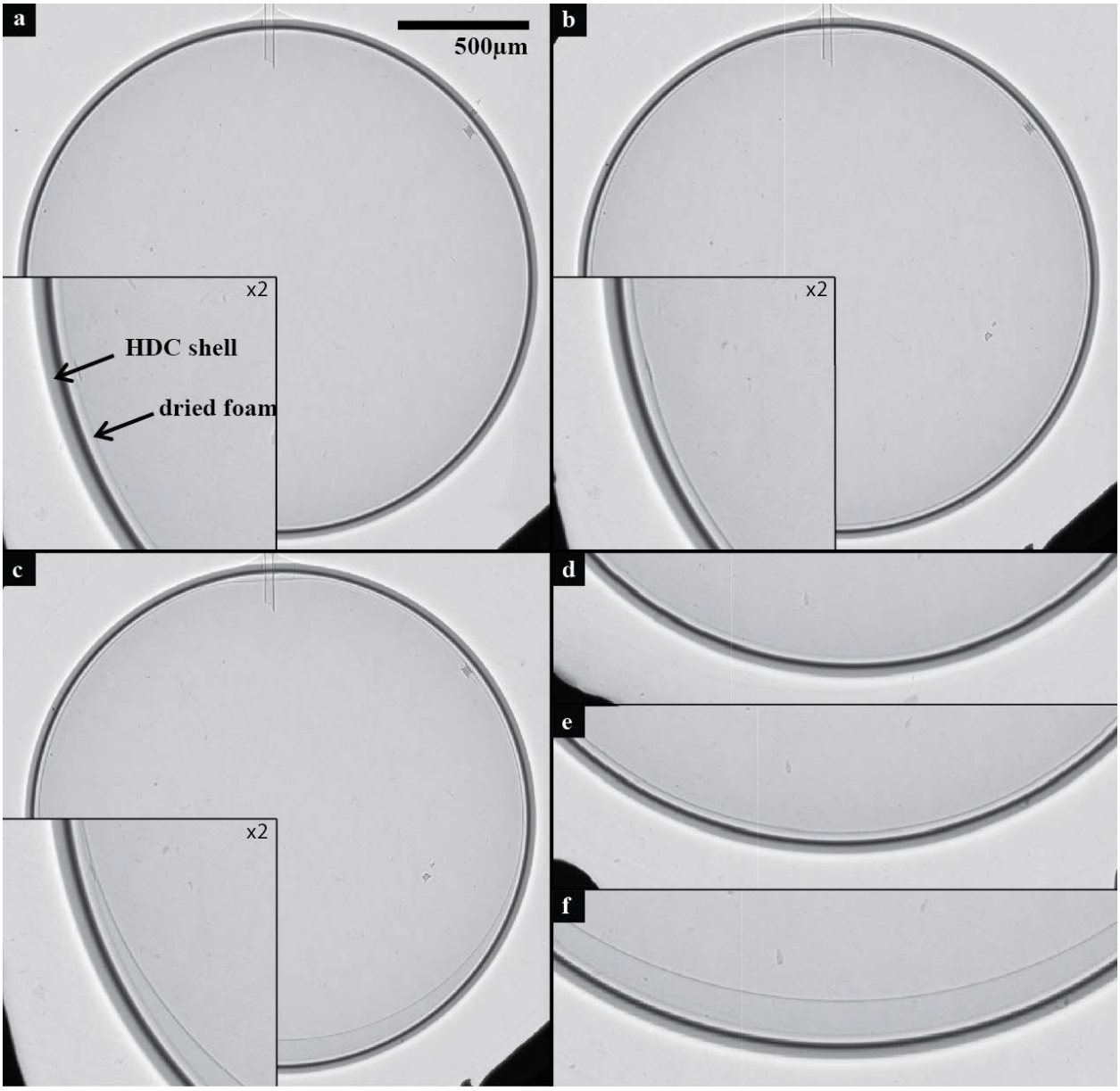

Figure 27: Wetting of 50 mg/cc iodine doped p-DCPD foam with liquid Deuterium: a) dry foam at room temperature without liquid deuterium; b) foam layering with liquid deuterium at 19.5 K; c) overfilling with liquid deuterium. The integrity of the foam is kept during the wetting with liquid Deuterium as we compare the close-up views of the dry foam (d), wet foam (e), and the overfilled capsule (f).

If more deuterium is inserted into the ablator shell, the liquid deuterium congregates at the bottom of the capsule, while the rest of the foam stays in its wetted state (figure 27c). The high resolution close-up views of the bottom part of the shell (figure 27d,e,f) reveal that the foam survives the wetting and is therefore suitable for deuterium layering. Not shown in the pictures is the freezing of the deuterium inside of the capsule, which was done every time during the overfilling. It did not do any damage to the foam, which maintained its structural integrity through the course of the entire experiment. The experiment was conducted multiple times to ensure reproducibility.

The deuterium wetting and freezing of the p-DCPD aerogel inside of the ICF target was done successfully and revealed that this aerogel is suited for layering experiments at the National Ignition Facility. Future experiments could analyze potential structural changes of the aerogel during the wetting process on length scales between 10^{-6}m to 10^{-10}m. *In situ* wetting experiments at the Advanced Photon Source at Argonne National Laboratory using Ultra Small Angle Scattering techniques could resolve such structural changes.

3 Summary and Outlook

During the research conducted for this thesis, the capability of p-DCPD aerogels to serve as a scaffold for deuterium and tritium inside of an ablator shell used at the National Ignition facility was analyzed and confirmed.

First, the compositions of different precursor solutions were tested and optimized to increase the uniformity of thin aerogel films inside of a vial. The optimal composition for a 25 mg/cc p-DCPD aerogel was found to be 15% norbornene and 0.2 wt.% Grubbs' 1st generation catalyst and for a 50 mg/cc aerogel 10% norbornene and 0.1w.% catalyst, whereas the thickness of the film doesn't seem to influence the uniformity of the coated aerogel. The thickness dependency was, however, somewhat inconclusive, since the repetition of the experiment lead to inconclusive results. The addition of a styrene-butadiene-styrene (SBS) block copolymer also does not appear to have a noticeable effect. Delaying the gelation of the precursor solution, however, gives the aerogel time to build up strength to withstand the shear forces during rotation, providing another possibility to improve the uniformity of the film layers. It was also found that a two-step polymerization of the precursor solution is not suitable for coating experiments of ICF-targets. The aforementioned results led to optimized coating conditions of p-DCPD aerogels, which were tested in high density carbon ablator shells.

For testing the aerogels inside of an ablator shell a filling standard was developed, which allows reproducibly injecting 0.1-1 µl of the precursor solution into the ablator. Weight gain measurements confirmed that the film layer thickness increases linearly with an applied pressure differential, independent of the hole diameter.

The filled capsules and the dried aerogels were analyzed with Ultra Small Angle Scattering (USAXS) at the Advanced Photon Source at Argonne National Laboratory. The aerogels withstand the wetting and

freezing with hydrogen and do not show any signs of structural change after being coated inside of an ablator shell or when exposed to the hydrogen.

Radiography results also confirmed that the dried aerogel layer inside of a high density carbon shell withstands the wetting and freezing with liquid deuterium. Additionally it was shown that the wetting of the foam occurs uniformly throughout the entire aerogel layer.

These experiments confirm that, with the examined composition, p-DCPD aerogels are feasible scaffolds for deuterium and tritium inside of ablator shells used at the National Ignition facility.

Future research could investigate the wetting of an aerogel layer inside of a high density carbon capsule with Ultra Small Angle X-ray techniques to examine potential changes on microscopic length scales during the exposure with deuterium and tritium. Furthermore different compositions of the precursor solution, which, for example, allow direct doping of the aerogel with different atoms, require further gelation experiments. The experimental techniques used during the research for this thesis will help characterize these newly developed compositions.

4 Acknowledgements

Many people have contributed to the successful completion of this thesis. First of all, I'd like to sincerely thank my thesis advisor Jürgen Biener, who supported my thesis at Lawrence Livermore National Laboratory. He was very supportive of my work and always provided me with direction and guidance.

I'd also like to thank my coworkers at LLNL Christoph Dawedeit, Kuang Jen Wu, Sung Ho Kim, Marcus Worsley, Monika Biener, Christopher Walton, Alexander Chernov, Trevor M. Willey, Tony van Buuren, Jon Lee, Joe Satcher, and my host Alex V. Hamza. They all helped me tremendously and made it a pleasure to work in this research group.

I want to thank Sibylle Günter, Scientific Director of the Max Planck Institut für Plasmaphysik, for being my advisor at the Technical University of Munich.

This work was performed under the auspices of the U. S. Department of Energy by Lawrence Livermore National Laboratory under Contract DE-AC52-07NA27344.

5 References

1. BP, *Energy Outlook 2030*. 2012.
2. Exxonmobil, *The Outlook for Energy: A View to 2040*. 2012.
3. WEO, *The IEA World Energy Outlook 2011*. 2011.
4. Khatib, H., *IEA World Energy Outlook 2011-A comment.* Energy Policy, 2012. **48**: p. 737-743.
5. Hoffert, M.I., et al., *Advanced technology paths to global climate stability: Energy for a greenhouse planet.* Science, 2002. **298**(5595): p. 981-987.
6. Nuckolls, J.H., *The Feasibility of inertial-confinement fusion.* Physics Today, 1982. **35**(9): p. 24-31.
7. Key, M.H., *Fast track to fusion energy.* Nature, 2001. **412**(6849): p. 775-776.
8. Moses, E.I., *The National Ignition Facility: Status and Progress towards Fusion Ignition.* Fusion Science and Technology, 2012. **61**(1T): p. 3-8.
9. Moses, E.I., *Ignition on the National Ignition Facility: a path towards inertial fusion energy.* Nuclear Fusion, 2009. **49**(10).
10. Nuckolls, J., et al., *Laser Compression of Matter to super-high densities - thermonuclear (CTR) applications.* Nature, 1972. **239**(5368): p. 139-&.
11. Rebut, P.H., et al., *Fusion Energy-Production from a Deuterium-Tritium Plasma in the JetTokamak.* Nuclear Fusion, 1992. **32**(2): p. 187-203.
12. Lawson, J.D., *Some criteria for a power producing thermonuclear reactor.* Proceedings of the Physical Society. Section B, 1957. **70**: p. 2-1010.
13. Lawson, J.D., *Power from Nuclear Fusion.* Nature, 1957. **180**(4590): p. 780-782.

14. Abdou, M.A., et al., *Conceptual design of a Tokamak reactor.* Texas Symposium on the Technology of Controlled Thermonuclear Fusion Experiments and the Engineering Aspects of Fusion Reactors. (Abstracts only received), 1972: p. 45-4545.

15. Spitzer, L., *THE STELLARATOR CONCEPT.* Physics of Fluids, 1958. **1**(4): p. 253-264.

16. Bol, K., et al., *Adiabatic compression of the Tokamak discharge.* 3rd International Symposium on Toroidal Plasma Confinement, 1973: p. B12/1 pp.-B12/1 pp.B12/1 pp.

17. Zwicker, H. and R. Wilhelm, *Toroidal confinement in screw pinches with non-circular plasma cross-section.* 5th European Conference on Controlled Fusion and Plasma Physics. Vol.I, 1972: p. 59-7070.

18. Alikaev, V.V., et al., *Investigation of HF plasma heating and of plasma behaviour in the TM-3 Tokamak.* 6th European Conference on Controlled Fusion and Plasma Physics. Vol.I, 1973: p. 63-6666.

19. Tenney, F.H., *PROBLEM IN PLASMA-FLOW INTO A TOKAMAK DIVERTOR.* Bulletin of the American Physical Society, 1972. **17**(11): p. 987-987.

20. Colven, C., A. Gibson, and P.E. Stott, *A local divertor for a Tokamak.* 5th European Conference on Controlled Fusion and Plasma Physics. Vol.II, 1972: p. 6-66.

21. Nuckolls, J., et al., *LASER IMPLOSION OF DT TO DENSITIES GREATER-THAN 1000 G/CM3 - OPTIMUM PULSE SHAPE - FUSION YIELD VS LASER ENERGY.* Bulletin of the American Physical Society, 1972. **17**(11): p. 1034-1035.

22. Freeman, J.R., et al., *Particle beam fusion research.* Nuclear Fusion, 1977. **1**: p. 167-175175.

23. Bluhm, H.J., G. Keßler, and R.R. Petersen, *Light ion beam driven inertial confinement fusion: Requirements and achievements.* Laser and Particle Beams, 1996. **14**(04): p. 655-663.

24. Arnold, R.C. and J. Meyer-ter-Vehn, *Inertial confinement fusion driven by heavy-ion beams.* Reports on Progress in Physics, 1987. **50**(5): p. 559.

25. Kuswa, G.W., *INERTIAL CONFINEMENT FUSION ENERGY WITH PARTICLE BEAMS.* Ieee Transactions on Nuclear Science, 1977. **24**(3): p. 975-980.

26. Metzler, N. and J. Meyertervehn, *TARGET STUDY FOR HEAVY-ION BEAM FUSION.* Laser and Particle Beams, 1984. **2**(FEB): p. 27-48.

27. Mason, R.J. and R.L. Morse, *TAMPED THERMONUCLEAR BURN OF DT-MICROSPHERES.* Nuclear Fusion, 1975. **15**(5): p. 935-938.

28. Afanasev, Y.V., et al., *THERMONUCLEAR LASER TARGETS WITH LARGE ENERGY GAIN COEFFICIENTS.* Nuclear Fusion, 1975: p. 119-121.

29. Mason, R.J. and R.L. Morse, *HYDRODYNAMICS AND BURN OF OPTIMALLY IMPLODED DEUTERIUM-TRITIUM SPHERES.* Physics of Fluids, 1975. **18**(7): p. 814-828.

30. Orth, C.D., *Relative Advantages of Direct and Indirect Drive for an Inertial Fusion Energy Power Plant Driven by a Diode-Pumped Solid-State Laser*. 2001. Medium: ED; Size: 9.

31. Suter, L., et al., *Feasibility of High Yield/High Gain NIF Capsules.* 1999.

32. Moses, E.I., et al., *A SUSTAINABLE NUCLEAR FUEL CYCLE BASED ON LASER INERTIAL FUSION ENERGY.* Fusion Science and Technology, 2009. **56**(2): p. 547-565.

33. Kucheyev, S.O. and A.V. Hamza, *Condensed hydrogen for thermonuclear fusion.* Journal of Applied Physics, 2010. **108**(9).

34. Atherton, J.L., *Targets for the National Ignition Campaign.* Journal of Physics: Conference Series, 2008. **112**(3): p. 032063 (4 pp.)-032063 (4 pp.)032063 (4 pp.).

35. Sacks, R.A. and D.H. Darling, *DIRECT DRIVE CRYOGENIC ICF CAPSULES EMPLOYING D-T WETTED FOAM.* Nuclear Fusion, 1987. **27**(3): p. 447-452.

36. Kim, N.K., et al., *Fabrication of hollow silica aerogel spheres by a droplet generation method and sol--gel processing.* Journal of Vacuum Science & Technology A: Vacuum, Surfaces, and Films, 1989. **7**(3): p. 1181-1184.

37. Paguio, R.R., et al., *Improving the wall uniformity of resorcinol formaldehyde foam shells by modifying emulsion components.* Fusion Science and Technology, 2007. **51**(4): p. 682-687.

38. Letts, S.A., et al., *Characterization of lowdensity foam materials for direct drive laser inertial confinement fusion targets.* Journal of Vacuum Science & Technology a-Vacuum Surfaces and Films, 1988. **6**(3): p. 1896-1897.

39. Takagi, M., et al., *Development of foam shell with plastic ablator for cryogenic laser fusion target.* Journal of Vacuum Science & Technology A: Vacuum, Surfaces, and Films, 1993. **11**(5): p. 2837-2845.

40. Takagi, M., et al., *Development of deuterated polystyrene shells for laser fusion by means of a density-matched emulsion method.* Journal of Vacuum Science & Technology A: Vacuum, Surfaces, and Films, 1991. **9**(4): p. 2145-2148.

41. Nikroo, A., et al., *Fabrication and properties of overcoated resorcinol-formaldehyde shells for omega experiments.* Fusion Science and Technology, 2004. **45**(2): p. 84-89.

42. Overturf, G.E., et al., *Resorcinol/formaldehyde foam shell targets for ICF.* Fusion Technology, 1995. **28**(5): p. 1803-1808.

43. Paguio, R.R., et al. *Fabrication Capabilities for Spherical Foam Targets Used in ICF Experiments*. in *Fusion Engineering 2005, Twenty-First IEEE/NPS Symposium on*. 2005.

44. Schroen-Carey, D., et al., *Hollow foam microshells for liquid-layered cryogenic inertial confinement fusion targets.* Journal of Vacuum Science & Technology A: Vacuum, Surfaces, and Films, 1995. **13**(5): p. 2564-2568.

45. Biener, J., et al., *A new approach to foam-lined indirect-drive NIF ignition targets.* Nuclear Fusion, 2012. **52**(6).

46. Lee, J.K. and G.L. Gould, *Polydicyclopentadiene based aerogel: a new insulation material.* Journal of Sol-Gel Science and Technology, 2007. **44**(1): p. 29-40.

47. Lenhardt, J.M., et al., *Increasing the oxidative stability of poly(dicyclopentadiene) aerogels by hydrogenation.* Polymer, 2013. **54**(2): p. 542-547.

48. Sakaiya, T., et al., *Ablative Rayleigh-Taylor instability at short wavelengths observed with moire interferometry.* Physical Review Letters, 2002. **88**(14).

49. Azechi, H., et al., *Comprehensive diagnosis of growth rates of the ablative Rayleigh-Taylor instability.* Physical Review Letters, 2007. **98**(4).

50. Knauer, J.P., et al., *Single-mode, Rayleigh-Taylor growth-rate measurements on the OMEGA laser system.* Physics of Plasmas, 2000. **7**(1): p. 338-345.

51. Pawley, C.J., et al., *Observation of Rayleigh-Taylor growth to short wavelengths on Nike.* Physics of Plasmas, 1999. **6**(2): p. 565-570.

52. Watari, T., et al., *Rayleigh-Taylor instability growth on low-density foam targets.* Physics of Plasmas, 2008. **15**(9).

53. Kim, S.H., et al., *Exploration of the versatility of ring opening metathesis polymerization: an approach for gaining access to low density polymeric aerogels.* Rsc Advances, 2012. **2**(23): p. 8672-8680.

54. Leventis, N., et al., *Polyimide Aerogels by Ring-Opening Metathesis Polymerization (ROMP).* Chemistry of Materials, 2011. **23**(8): p. 2250-2261.

55. Davidson, T.A., K.B. Wagener, and D.B. Priddy, *Polymerization of dicyclopentadiene: A tale of two mechanisms.* Macromolecules, 1996. **29**(2): p. 786-788.

56. Davidson, T.A. and K.B. Wagener, *The polymerization of dicyclopentadiene: an investigation of mechanism.* Journal of Molecular Catalysis a-Chemical, 1998. **133**(1-2): p. 67-74.

57. Schwab, P., R.H. Grubbs, and J.W. Ziller, *Synthesis and Applications of RuCl2(CHR')(PR3)2: The Influence of the Alkylidene Moiety on Metathesis Activity.* J. Am. Chem. Soc., 1996. **118**(1): p. 100-110.

58. Dawedeit, C., et al., *Tuning the rheological properties of sols for low-density aerogel coating applications.* Soft Matter, 2012.

59. Melo, F., *Localized states in a film-dragging experiment.* Physical Review E, 1993. **48**(4): p. 2704-2712.

60. Dawedeit, C., et al., *Coating functional sol–gel films inside horizontally-rotating cylinders by rimming flow/state.* Journal of Sol-Gel Science and Technology, 2012: p. 1-8.

61. Seiden, G. and P.J. Thomas, *Complexity, segregation, and pattern formation in rotating-drum flows.* Reviews of Modern Physics, 2011. **83**(4): p. 1323-1365.

62. Thoroddsen, S.T. and L. Mahadevan, *Experimental study of coating flows in a partially-filled horizontally rotating cylinder.* Experiments in Fluids, 1997. **23**(1): p. 1-13.

63. *Script correction fluid used in image forming appts. - obtd. by dispersing at least binding resins, white pigments and pale colouring agent in volatile solvents*, Mita Ind C0 Ltd (Mtai).

64. Letts, S.A., et al., *Structure and Properties of Resorcinol-Formaldehyde Gels.* MRS Online Proceedings Library, 1989. **177**: p. null-null.

65. Biener, J., et al., *Diamond spheres for inertial confinement fusion.* Nuclear Fusion, 2009. **49**(11).

66. Reichenauer, G., et al., *In-situ monitoring of the deformation of nanopores due to capillary forces upon vapor sorption.* HMI Annual Report 2008, 2008.

67. Balzer, C., et al., *Deformation of Porous Carbons upon Adsorption.* Langmuir, 2011. **27**(6): p. 2553-2560.

68. Reichenauer, G. and G.W. Scherer, *Nitrogen sorption in aerogels.* Journal of Non-Crystalline Solids, 2001. **285**(1-3): p. 167-174.

69. Leachman, J.W., et al., *Fundamental Equations of State for Parahydrogen, Normal Hydrogen, and Orthohydrogen.* Journal of Physical and Chemical Reference Data, 2009. **38**(3).

70. Fan, Z. and J. Ilavsky, *Ultra-small-angle X-ray Scattering of Polymers.* Polymer Reviews, 2010. **50**(1): p. 59-9090.

71. Ilavsky, J., et al., *Ultra-small-angle X-ray scattering at the Advanced Photon Source.* Journal of Applied Crystallography, 2009. **42**: p. 469-479.

72. Long, G.G., et al., *HIGH-RESOLUTION SMALL-ANGLE X-RAY-SCATTERING CAMERA FOR ANOMALOUS SCATTERING.* Journal of Applied Crystallography, 1991. **24**: p. 30-37.

73. Ilavsky, J. and P.R. Jemian, *Irena: tool suite for modeling and analysis of small-angle scattering.* Journal of Applied Crystallography, 2009. **42**: p. 347-353.

74. Chubb, J.N., L. Gowland, and I.E. Pollard, *Condensation pumping of hydrogen and deuterium on to liquid-helium-cooled surfaces.* British Journal of Applied Physics (Journal of Physics D), 1968. **1**: p. 361-370370.

75. Koch, J.A., et al., *Refraction-enhanced x-ray radiography for inertial confinement fusion and laser-produced plasma applications.* Journal of Applied Physics, 2009. **105**(11).

76. Kozioziemski, B.J., et al., *Quantitative characterization of inertial confinement fusion capsules using phase contrast enhanced x-ray imaging.* Journal of Applied Physics, 2005. **97**(6).

77. Wilkins, S.W., et al., *Phase-contrast imaging using polychromatic hard X-rays.* Nature, 1996. **384**(6607): p. 335-338.

78. Grilly, E.R., *THE VAPOR PRESSURES OF HYDROGEN, DEUTERIUM AND TRITIUM UP TO 3 ATMOSPHERES.* Journal of the American Chemical Society, 1951. **73**(2): p. 843-846.

79. Friedman, A.S., D. White, and H.L. Johnston, *THE DIRECT DETERMINATION OF THE CRITICAL TEMPERATURE AND CRITICAL PRESSURE OF NORMAL DEUTERIUM - VAPOR PRESSURES BETWEEN THE BOILING AND CRITICAL POINTS.* Journal of the American Chemical Society, 1951. **73**(3): p. 1310-1311.